VqERF1B-VqERF062-*VqNSTS2* transcriptional cascade enhances stilbene biosynthesis and resistance to powdery mildew in grapevine

Chaohui Yan[1,2,3,†], Wandi Liu[1,2,3,†], Ruimin Li[1,2,3], Guotian Liu[1,2,3,*] and Yuejin Wang[1,2,3,*] (iD)

[1]*College of Horticulture, Northwest A & F University, Yangling, Shaanxi, China*

[2]*Key Laboratory of Horticultural Plant Biology and Germplasm Innovation in Northwest China, Ministry of Agriculture, Yangling, Shaanxi, China*

[3]*State Key Laboratory of Crop Stress Biology in Arid Areas, Northwest A & F University, Yangling, Shaanxi, China*

Summary

Grapes, as one of the world's oldest economic crops, are severely affected by grape powdery mildew, causing significant economic losses. As a phytoalexin against powdery mildew, stilbenes and their key synthetic gene, *stilbene synthase* (*STS*), are highly sought after by researchers. In our previous research, a new gene, *VqNSTS2*, was identified from *Vitis quinquangularis* accession 'Danfeng-2' through transcriptomic analysis. However, the function and molecular mechanism of *VqNSTS2* gene remain unknown. Here, by characterization and transient overexpression of *VqNSTS2*, we demonstrated that its expression product, stilbenes, can be detected in the model plant tobacco, which does not inherently contain *STSs*. After artificially inoculating transgenic Arabidopsis lines overexpressing *VqNSTS2* with *Golovinomyces cichoracearum*, it was found that *VqNSTS2* actively moved to the pathogen's haustorium after responding to the pathogen, recognized and enveloped the haustorium, blocking the pathogen's infection and invasion and exhibited disease resistance. Furthermore, *Agrobacterium*-mediated stable overexpression of *VqNSTS2* promoted stilbene accumulation and enhanced resistance of the *V. vinifera* susceptible cultivar 'Thompson Seedless' to *E. necator*. Additionally, through screening and identification, a transcription factor, VqERF062, was found to directly bind to the DRE and RAA motifs on ProVqNSTS2, positively regulating *VqNSTS2* expression. Moreover, VqERF062 directly interacted with VqERF1B to promote the transcription of *VqNSTS2* in addition to forming a homodimer with itself. Taken together, our findings reveal that the VqERF1B-VqERF062- module is required for grape resistance to *E. necator* and providing insights into the regulatory mechanism of stilbenes biosynthesis. [Correction added on 22 March 2025, after first online publication: The 7th sentence in summary is updated in this version.].

Introduction

Grapevine (*Vitis vinifera* L.) is an agriculturally and economically important fruit crop and is widely cultivated for its excellent flavour of the berries, but it is very susceptible to powdery mildew (PM) caused by *Erysiphe necator* (previously *Uncinula necator*) (Qiu et al., 2015). When plants suffering from pathogens, a two-tiered immune system: PAMP-Triggered Immunity (PTI) and Effector-Triggered Immunity (ETI) was stimulated as a unified system (Jones and Dangl, 2006; Pruitt et al., 2021). For grapevine, it is manifested as the deposition of callose, the accumulation of reactive oxygen species (ROS) and stilbenes and the hypersensitive reaction (HR)-like cell death (Hu et al., 2021; Li et al., 2025; Qiu et al., 2015; Ramming et al., 2010; Yin et al., 2022).

Stilbenes, an important phenolic plant secondary metabolites, are a kind of naturally occurring phytoalexin that protect plants from PM (Xu et al., 2019a). Resveratrol (3,5,4'-trihydroxystilbene), is the basic unit of stilbenes in grapevine, which usually functions as an antimicrobial compound in plants (Schnee et al., 2008). In addition, resveratrol has pharmacological properties, which is beneficial to human health, such as anti-cancer, anti-tumour,

anti-oxidative and anti-inflammatory (Jang et al., 1997). Stilbene synthase (STS; EC2.3.1.95) catalyses the biosynthesis of resveratrol from three molecules of malonyl CoA and one molecule of hydroxycinnamoyl CoA *via* the phenylalanine/polymalonates pathway (Chong et al., 2009). The first enzymes of phenylalanine/polymalonates pathway is phenylalanine ammonia lyase (PAL). STS and chalcone synthase (CHS; EC 2.3.1.74) share highly conserved sequence and compete the same substrates in the last step (Schöppner and Kindl, 1984). In 2007, the grape genome of 'PN40024' was published (Jaillon et al., 2007). STS gene family was identified to contain 48 members and located on two chromosomes, 10 and 16 (Parage et al., 2012; Vannozzi et al., 2012). A large number of studies have demonstrated that the homologous or heterologous overexpression of *STS* gene can promote stilbenes accumulation and enhance disease resistance, including *E. necator* (Dai et al., 2015; Huang et al., 2016; Liu et al., 2019; Wang et al., 2017), *Botrytis cinerea* (Coutos-Thévenot et al., 2001; Hain et al., 1993; Huang et al., 2018; Leckband and Lörz, 1998; Vishnevetsky et al., 2011; Wang et al., 2017), *Pyricularia oryzae* (Stark-Lorenzen et al., 1997), *Puccinia recondita* and *Septoria nodorum* (Coutos-Thévenot et al., 2001).

Stilbene synthases responses to *E. necator* have been well studied; however, the transcriptional regulation of *STSs* is more elusive and complex. At present, the research on transcription regulation of *STSs* mainly focuses on MYB and WRKY transcription factor families. VvMYB14 and VvMYB15 were reported to specifically activate the promoters of *STSs* by transient gene reporter assays (Höll *et al.*, 2013). Then MYB14 was demonstrated to directly bind to the Box-L5 motif in the promoters of *STSs* (Fang *et al.*, 2014). VviMYB13 also played a crucial role in regulating stilbene accumulation because it shares common co-expressed *STSs* with VviMYB14 and VviMYB15 (Wong *et al.*, 2016). VqMYB35 could activate the expressions of *VqSTSs* by binding directly to the MBS elements in *STS* promoters (Wang and Wang 2019b). VqMYB154 was confirmed to activate the *VqSTSs* by directly binding to their promoters (Jiang *et al.*, 2021). Besides, a study showed that MYB14, MYB15 and MYB13 bind to 30 out of 47 *STS* genes (Orduña *et al.*, 2022). VqWRKY31 could activate the expression of *STS9* and *STS48* by directly bind to their promoters (Yin *et al.*, 2022). Furthermore, MYB and WRKY can also form protein complexes to coordinate the regulation of *STS* expression. For instance, Vannozzi *et al.* (2018) found that WRKY were the top TF family correlated with *STSs*; and suggested that VviWRKY24 could activate the *VviSTS29* promoter as a singular effector, while VviWRKY03 acts through a combinatorial effect with VviMYB14. VqWRKY53 could activate the expression of *STSs*; and the regulatory functions to *STSs* showed stronger when co-expressed with VqMYB14 and VqMYB15 (Wang *et al.*, 2020a). In addition, VvMYB14-VvWRKY8-VvMYB30 complex was demonstrated to produce stilbenes and prevent excessive accumulation of stilbenes to balance metabolic costs (Jiang *et al.*, 2019; Mu *et al.*, 2023). Additionally, other transcription factors have also been reported to be involved in transcriptional regulation of *STSs*. For instance, VqbZIP1 interacts with VqSnRK2.4 or VqSnRK2.6 exhibiting higher activation efficiency to the *STS* promoters (Wang and Wang, 2019a). VqAL4 can directly bind to the G-rich element (CACCTC) in the *VqNSTS4* promoter and activate its expression (Yan *et al.*, 2023). However, there are few reports that other transcription factors regulate *STSs* expression.

The APETALA2/E thylene Responsive Factor (AP2/ERF) family is one of the most important TF superfamilys in plant and play key roles in plant growth and development, biotic and abiotic stresses, such as root growth, fruit ripening, low temperature, drought, high salt, *B. cinerea* (Chen *et al.*, 2022; Hong *et al.*, 2022; Wang *et al.*, 2021; Xiang *et al.*, 2025; Zhuang *et al.*, 2021). In addition, a large number of studies have demonstrated that AP2/ERF subfamily is involved in regulating metabolites biosynthesis, including artemisinin, *E*-geraniol, lignan/lignin, tanshinone, flavonoid and carotenoid (Li *et al.*, 2017; Ma *et al.*, 2017; Tan *et al.*, 2015; Zhao *et al.*, 2021; Zheng *et al.*, 2021; Zhu *et al.*, 2021). However, there are only one report that VqERF114 increased *VqSTS* expression and stilbene accumulation by interacting with VqMYB35 (Wang and Wang 2019b). The potential role of AP2/ERF in transcriptional regulation of *STSs* is largely unexplored.

China is one of origin centres of grapevine, and it possesses abundant wild grape germplasm resources (Atak, 2024). The Chinese wild *V. quinquangularis* accession 'Danfeng-2' has received extensive attention due to its high resistance to PM and high levels of stilbenes (Shi *et al.*, 2014; Zhou *et al.*, 2015). Recently, six novel *STS* transcripts (named *VqNSTS1-6*) were identified through the transcriptome (PRJNA306731) of 'Danfeng-2' (Li, 2019). Furthermore, *VqNSTS3* and *VqNSTS4* have

been shown to enhance grape disease resistance by regulating different disease-resistance pathways, particularly *VqNSTS3*, which prevents pathogen invasion in model plant Arabidopsis by encapsulating the pathogen's haustoria (Liu *et al.*, 2023; Yan *et al.*, 2023). Here, we demonstrated that *VqNSTS2* promotes the accumulation of stilbenes and increases resistance to PM in susceptible grapevines. Moreover, VqERF062 activates *VqNSTS2* by directly binding to its promoter and forms the VqERF1B-VqERF062 complex to further promote *VqNSTS2* expression, which results in the resistance to PM in grapevines. The aim of this study was to reveal the molecular regulatory mechanism of *VqNSTS2* and to provide basis for grape breeding against PM in the future.

Results

VqNSTS2 has conserved motifs of the stilbene synthase gene family and exhibits induced expression after artificial inoculation with *E. necator*

In our previous study, we identified six new STS members from Chinses wild *V. quinquangularis* accession 'Danfeng-2', which play important roles in the synthesis of stilbenes and the *E. necator* response (Figure S1 and Table S1) (Yan *et al.*, 2023). The full-length coding sequence (CDS) of *VqNSTS2* (GenBank accession No. OL589477) is 1179 bp and encoded a protein with 392 amino acids (aa) (Figure 1a); and showed 98.73% similarity to *VvSTS46* from *V. vinifera* 'PN40024 (Figure 1b). Protein sequence analysis revealed that VqNSTS2 contains the conserved STS family domains and showed 99.49% aa sequence identity with VqSTS37 (Figure 1c,d), indicating that VqNSTS2 belongs to STS family. Subcellular localization analysis in Arabidopsis protoplast showed that the green fluorescence signal of VqNSTS2-GFP was existed in the cytoplasm (Figure 1e). To test whether VqNSTS2 has enzymatic activity, it was overexpressed in tobacco, which is a model plant without *STS* gene. The results found that the transient overexpression of *VqNSTS2* in tobacco leaves can lead to the production of stilbenes, indicating that VqNSTS2 has stilbenes synthase activity (Figure 1f). Under artificial inoculation with *E. necator*, the expression of *VqNSTS2* was rapidly and significantly up-regulated and then gradually down-regulated (Figure 1g), suggesting that it may function in the early stage of the PM response.

VqNSTS2 transgenic *Arabidopsis thaliana* lines enhance resistance to *Golovinomyces cichoracearum* through expression *VqNSTS2* encapsulating the fungus haustoria to prevent pathogen invasion

A. thaliana is a model plant without *STS* gene inherently, so it is suitable to studying the function of *STS* gene. To investigate the contribution of *VqNSTS2* to powdery mildew, we generated transgenic *A. thaliana* lines for *ProVqNSTS2*::VqNSTS2-GFP through *Agrobacterium*-mediated transformation (Figure 2a,b). As shown in Figure 2c, the leaves of *ProVqNSTS2*::VqNSTS2-GFP transgenic lines were only observed limited whitish fungal mass after artificially inoculated with *G. cichoracearum*. As the control, the leaves of Col-0 lines were covered with white mycelia after artificially inoculated with *G. cichoracearum* (Figure 2c). Trypan blue, DAB and NBT staining of infected leaves at 7 days post inoculation (dpi) revealed that most epidermal cells containing haustoria of *G. cichoracearum* underwent HR cell death as evidenced by massive H_2O_2 accumulation and dark blue stains indicative of cell death, respectively (Figure 2d). By contrast, there
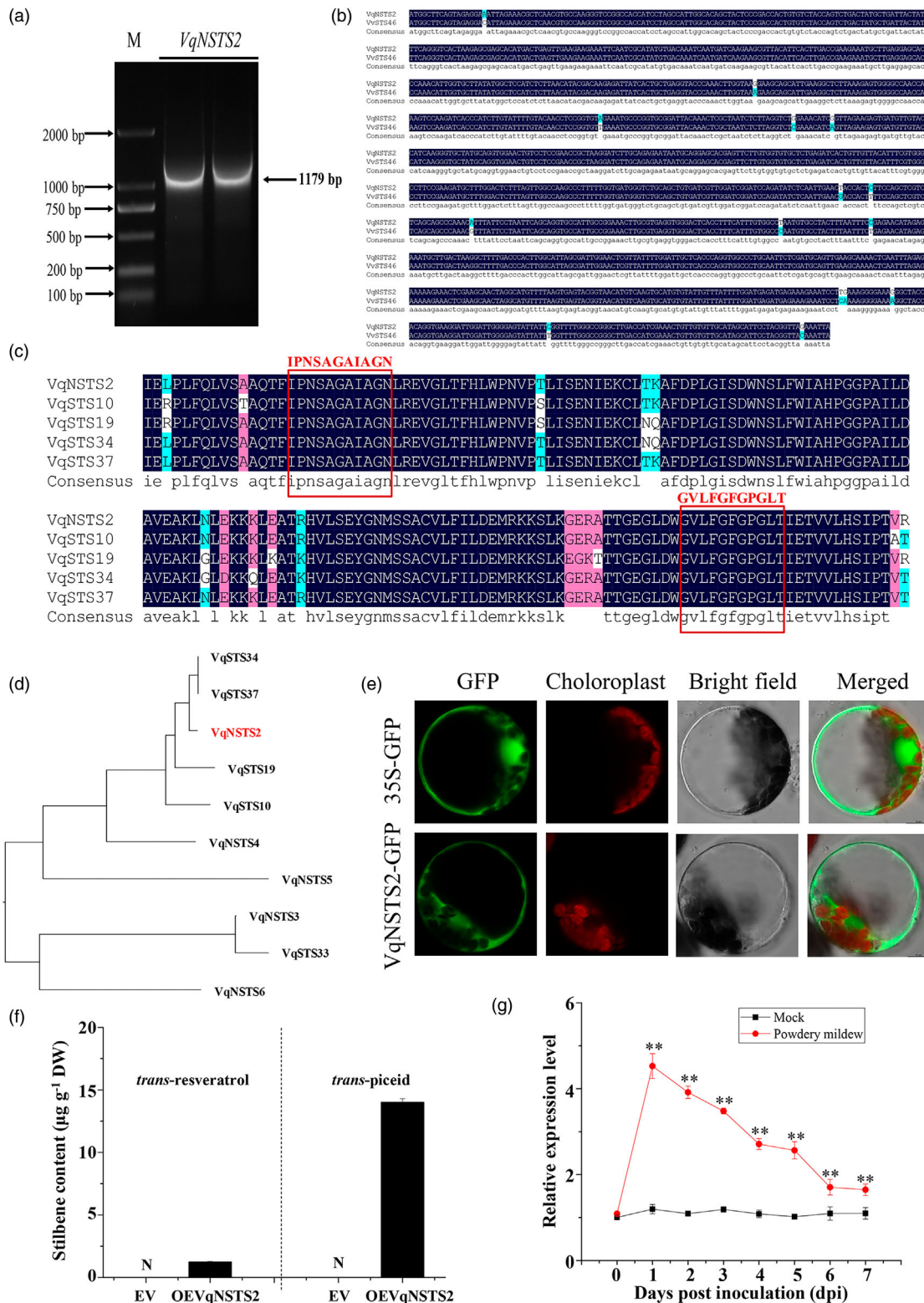
Figure 1 Cloning and expression analysis of *VqNSTS2* under *Erysiphe necator* artificial inoculation in grapevine. (a) Amplification of *VqNSTS2* from Chinese wild *V. quinquangularis* accession 'Danfeng-2'. (b) DNA sequence alignment between *VqNSTS2* and *VvSTS46* (XM_002263686). (c) Sequences alignment of conserved domain of VqNSTS2 and other VqSTS proteins in 'Danfeng-2'. The red boxes indicate the STS family conserved domains. (d) Phylogenetic analysis of VqNSTS2 and part of VqSTSs from 'Danfeng-2'. VqNSTS2 is highlighted in red. (e) Subcellular localization of VqNSTS2-GFP in Arabidopsis protoplast. Bars = 10 μm. (f) The content of stilbenes after transient overexpression of *VqNSTS2* in tobacco. (g) Expression analysis of *VqNSTS2* in 'Danfeng-2' leaves under artificial inoculation with *E. necator*. dpi: days post inoculated with *E. necator*. The standard deviation (SD) was calculated from three biological replicates. Asterisks indicate significant differences (**$P < 0.01$, Student's *t* test).
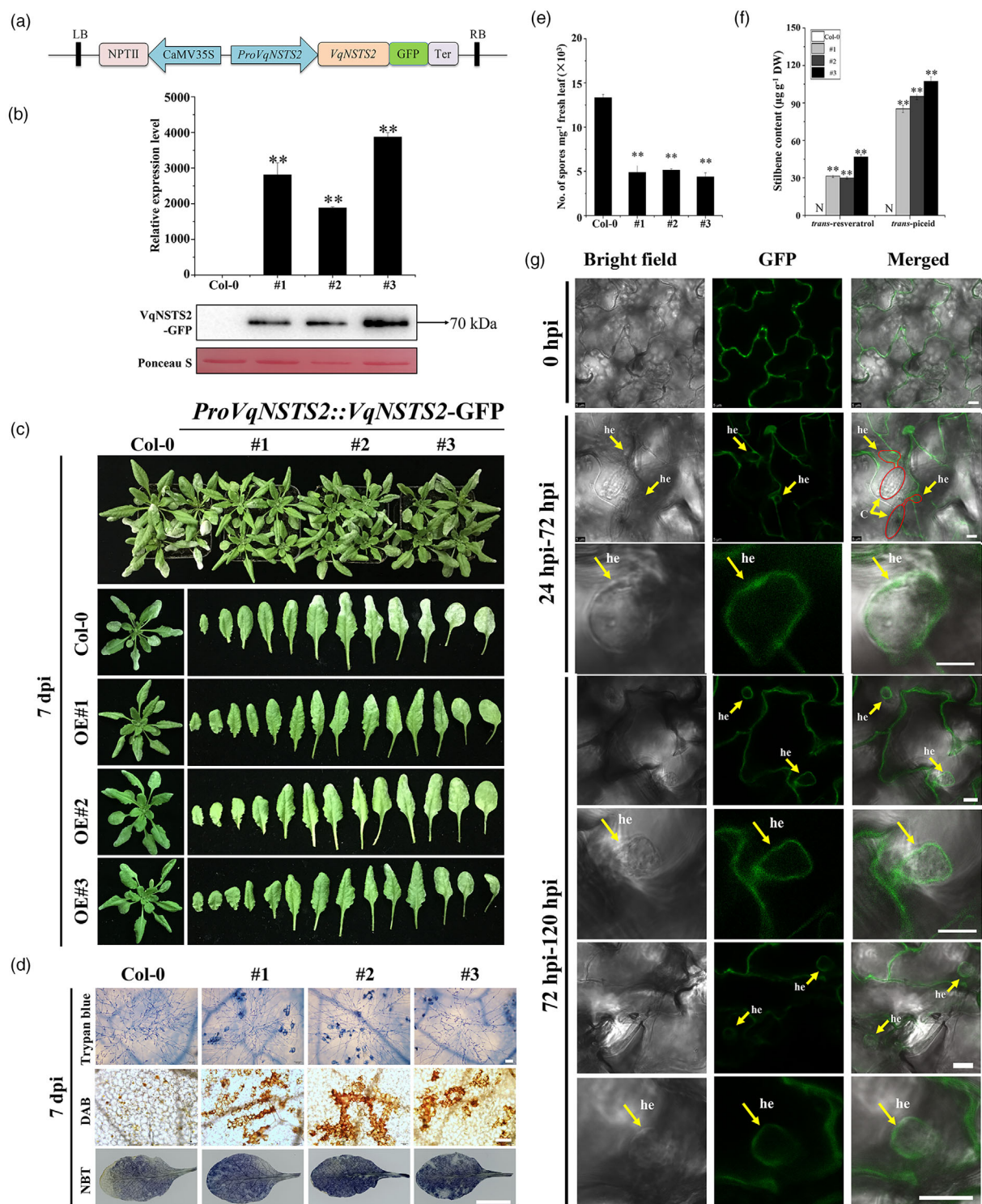
Figure 2 Functional characterization of *VqNSTS2* in regulating powdery mildew tolerance in transgenic *Arabidopsis*. (a) Schematic diagram of *ProVqNSTS2*::VqNSTS2-GFP vector. (b) Expression analysis of *VqNSTS2* in *ProVqNSTS2*::VqNSTS2-GFP transgenic *Arabidopsis* lines. (c) Representative *ProVqNSTS2*::VqNSTS2-GFP transgenic *Arabidopsis* lines and Col-0 at 7-days post inoculated (dpi) with *Golovinomyces cichoracearum*. (d) Histochemical staining of *ProVqNSTS2*::VqNSTS2-GFP transgenic *Arabidopsis* lines and Col-0 leaves at 7 dpi stained with trypan blue, diaminobenzidine staining (DAB) and nitroblue tetrazolium chloride (NBT). Upper and middle figures bars = 100 μm and lower figures bars = 1 cm. (e) Quantification of spores per mg fresh leaves from *ProVqNSTS2*::VqNSTS2-GFP transgenic *Arabidopsis* lines and Col-0 at 7 dpi. (f) Stilbenes contents in the leaves of *ProVqNSTS2*::VqNSTS2-GFP transgenic *Arabidopsis* lines and Col-0 at 7 dpi. One-way ANOVA (Tukey's test) was performed and asterisks indicate significant differences at **$P < 0.01$. (g) Confocal microscope images from single optical sections of *Arabidopsis* leaf epidermal cells expressing *ProVqNSTS2*::VqNSTS2-GFP infected by *G. cichoracearum*. The middle column shows *ProVqNSTS2*::VqNSTS2-GFP fluorescence and the right column shows the merged field images. hpi: hours post inoculation; he, haustorial encasement; C, conidium. Bars = 5 μm.

Table 1 Content of stilbenes of *VqNSTS2* transgenic *Arabidopsis* after artificial inoculation with *Golovinomyces cichoracearum* by HPLC analysis

Lines	*Trans*-resveratrol (μg/g)	*Trans*-piceid (μg/g)
Col 0–7 dpi	Null	Null
ProVqNSTS2::*VqNSTS2* #1–7 dpi	31.50 ± 1.21	85.27 ± 2.92
ProVqNSTS2::*VqNSTS2* #2–7 dpi	29.95 ± 0.84	95.29 ± 2.49
ProVqNSTS2::*VqNSTS2* #3–7 dpi	46.78 ± 1.91	107.37 ± 3.70

Table 2 Content of stilbenes of *VqNSTS2* transgenic mutants under natural conditions and after artificial inoculation with *Erysiphe necator* by HPLC

Lines	*Trans*-resveratrol (μg/g)	*Trans*-piceid (μg/g)	ε-viniferin (μg/g)
WT	37.52 ± 9.01	129.78 ± 9.51	16.95 ± 3.25
OEVqNSTS2 OE#2	105.33 ± 16.74	323.98 ± 34.77	36.55 ± 7.19
OEVqNSTS2 OE#4	120.62 ± 13.25	400.46 ± 30.04	37.46 ± 8.34
WT-7 dpi	53.3 ± 7.16	146.9 ± 12.01	24.11 ± 4.81
OEVqNSTS2 OE#2–7 dpi	131.36 ± 16.43	447.65 ± 23.59	51.64 ± 5.26
OEVqNSTS2 OE#4–7 dpi	182.45 ± 11.39	497.92 ± 26.93	63.38 ± 6.36
EV	130.99 ± 1.60	313.73 ± 2.28	24.22 ± 0.74
RNAi*VqNSTS2/STS37*	74.41 ± 20.95	133.10 ± 58.43	9.39 ± 3.88

was less HR cell death and H_2O_2 accumulation in the infected leaves of Col-0 plants (Figure 2d). Spore quantification of infected mature leaves at 7 dpi showed that plants of *ProVqNSTS2*::VqNSTS2-GFP transgenic lines produced much less (~30%) spores compared to those of the Col-0 plants (Figure 2e). In addition, *trans*-resveratrol and piceid were detected in *ProVqNSTS2*::VqNSTS2-GFP transgenic lines at 7 dpi (Figure 2f and Table 1). In order to further found the direct evidence of *VqNSTS2* resistance to powdery mildew, we used laser confocal microscopy to observe the accumulation of green fluorescence in *ProVqNSTS2*::VqNSTS2-GFP transgenic lines after artificially inoculated with *G. cichoracearum*. As shown in Figure 2g, the green fluorescence of *ProVqNSTS2*::VqNSTS2-GFP started to accumulate at the invasion site of *G. cichoracearum*. In addition, with the invasion time increased the haustorium was formed and the green fluorescence was observed accumulated around the haustorium and a cup-shaped encasement begin to form around the haustorium (24–72 hpi). Then, the green fluorescence completely encrusted the haustorium to form the encasement after artificially inoculated with *G. cichoracearum*. At 72–120 hpi green fluorescence accumulation was observed around the secondary haustorium (Figure 2g). The above results proved that stilbene synthase could directly respond and interact with fungi to form the physical barrier to inhibit the germination and invasion of spores.

VqNSTS2 transgenic grapevine lines show enhanced resistance to *E. necator* and activation of resistance-related genes

To investigate the contribution of *VqNSTS2* to *E. necator*, we generated transgenic grapevine plants for *35S-VqNSTS2-GFP* through *Agrobacterium*-mediated transformation of pro-embryogenic masses derived from 'Thompson Seedless' (Figure S2). Western blot assays showed that the VqNSTS2-GFP fusion protein were expressed in six transgenic grapevine plants (Figure S2C). Among these transgenic grapevine plants, we selected two high-expressed overexpression transgenic lines (OE#2 and OE#4) to conducted the further study (Figure S2E,F). To test the effect of *VqNSTS2* overexpression on the phenylalanine/polymalonates pathway, we quantified the transcriptional level of these three genes including *PAL*, *STS* and *CHS*. As shown in Figure S2E, compared with the wild type plants (WT), the expression levels of three genes in *VqNSTS2* transgenic plants all increased significantly, and the increase of *STS* transcription level was obviously higher than that of *CHS* transcription level. As the downstream products of *STS*, stilbenes were detected by HPLC in transgenic plants and WT. The results showed that the content of stilbenes in two transgenic lines increased significantly (Figure S2F and Table 2).

To assess the resistance to *E. necator*, OE lines and WT were inoculated with grapevine *E. necator*. As shown in Figure 3b, the leaves of OE lines appeared fewer fungal spores colonies at 7 dpi. Trypan blue, scanning electron micrographs and quantification of the number of spores revealed the relatively slow hypha growth on the leaves of OE lines (Figure 3c,d,f). At the same time, massive H_2O_2, callose deposition and HR-like cell death was also observed in OE lines but not WT (Figure 3d,e,g). Stilbenes content and transcriptional levels of resistance-related genes in the two OE lines increased more times than that in WT (Figure 3h,i and Table 2). In addition, we conducted an RNA interference (RNAi) approach to investigate the resistance to *E. necator* in transiently transformed Danfeng-2 leaves (Figure 3j–l). Because of the high sequences similarity of *VqNSTS2* and *VqSTS37*, we can only interfere with *VqNSTS2* and *VqSTS37* at the same time. However, RNAi-*VqNSTS2/STS37* in 'Danfeng-2' showed the opposite results compared with OE plants (Figure 3m–p and Table 2). Taken together, the above results indicated that *VqNSTS2* could positively regulate resistance to PM in grapevine by accumulating more stilbenes and activating various resistance genes.

VqERF062 upregulates the expression of *VqNSTS2* and the accumulation of stilbenes and enhances the resistance to PM

Co-expression analysis was carried out using the RNA-seq data (PRJNA306731) of 'Danfeng-2' to find the potential regulation factors involved in the transcription of *VqNSTS2*. Pearson's correlation coefficient (PCC) represented the degree of co-expression relationship (Sedgwick, 2012). Eight potential regulation factors were obtained with PCC ≥0.89 (Figure S3A and Table S2). Dual Luciferase assay was used to compare the activation effect on the promoter of *VqNSTS2* of eight potential regulation factors. Finally, an ERF transcription factor, *VqERF062* (VIT_05s0029g00140), was identified as a stronger regulation factor (Figure S3B,C). *VqERF062* was predicted to be located on chromosome 5 and contained a AP2 domain (residues 265–328 aa) (Figure S4A,B). Cluster analysis of VqERF062 and its homologous proteins from other species showed that VqERF062 shows high homology with VvERF062 and VrERF062 (Figure S4C). VqERF062 which is located in the nucleus, responded to PM and peaked at 4 dpi (Figure S4D,E).

To determine the regulation between VqERF062 and *VqNSTS2*, dual luciferase assay were carried out. The fusion vectors, ProVqNSTS2-Luc, containing the reporter gene luciferase were
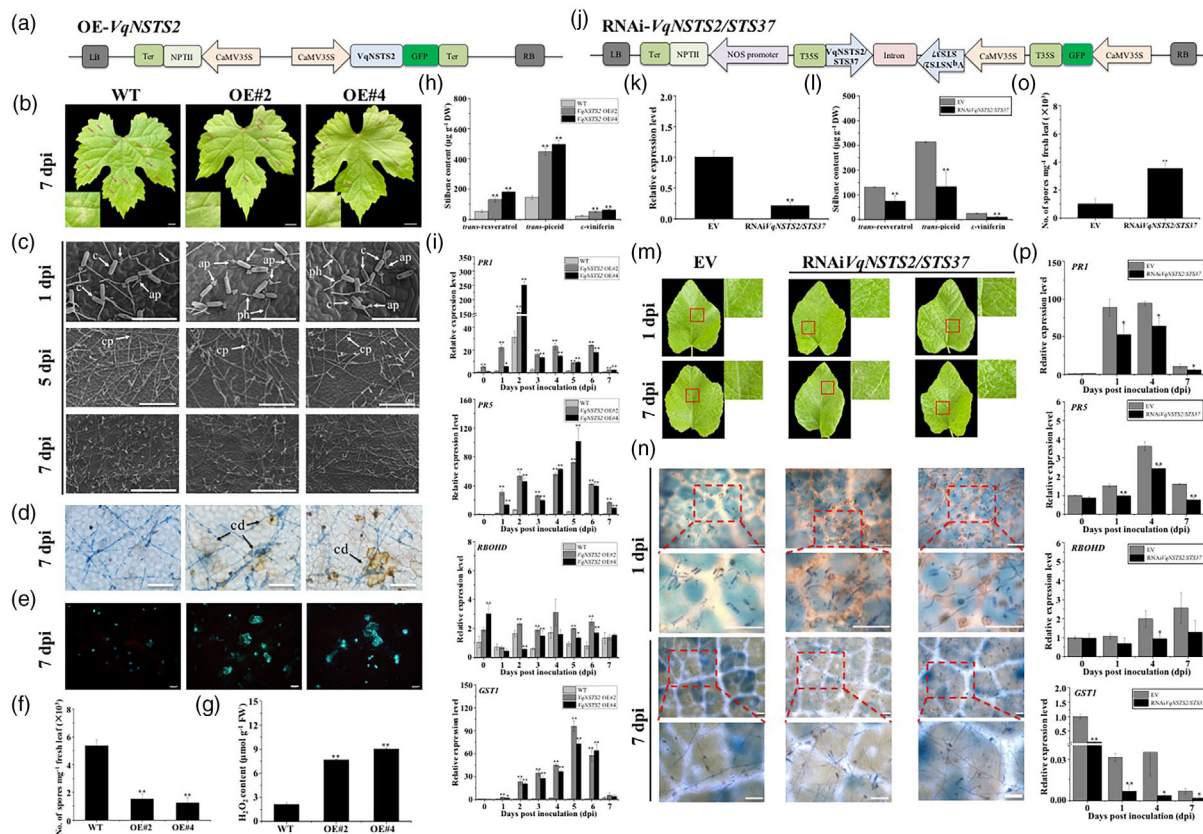
Figure 3 Transgenic *VqNSTS2* grapevine plants show enhanced resistance to *Erysiphe necator*. (a) Schematic diagram of the 35S-VqNSTS2-GFP construct. (b) Photograph of leaves of two overexpression transgenic plants (OE) and wild type 'Thompson Seedless' (WT) at 7-days post inoculated (dpi) with *E. necator* (c) Scanning electron micrographs of the hyphae of *E. necator* in OE and WT plants. Upper figures bars = 100 μm, middle figures bars = 200 μm and lower figures bars = 500 μm. (d) Histochemical staining of OE and WT plants leaves at 7 dpi stained with trypan blue and diaminobenzidine staining (DAB). Bars = 50 μm. (e) Aniline blue staining shows the callose depositions at 7 dpi. Bars = 50 μm. (f) Quantification of spores per mg fresh leaves from OE and WT plants at 7 dpi. (g) H$_2$O$_2$ content of OE and WT plants leaves at 7 dpi. (h) Stilbenes contents in the leaves of OE and WT plants at 7 dpi. (i) qRT-PCR analysis of resistance-related genes in OE and WT plants after *E. necator* inoculation. One-way ANOVA (Tukey's test) was performed and asterisks indicate significant differences at *$P < 0.05$, **$P < 0.01$. (j) Schematic diagram of the RNAi-VqNSTS2/STS37-GFP construct. (k) Relative transcript levels of *VqNSTS2* in RNAi*VqNSTS2/STS37* lines and empty vector (EV) grapevine leaves. (l) Stilbenes contents in the leaves of RNAi*VqNSTS2/STS37* lines and EV grapevine leaves. (m) Photograph of leaves of RNAi*VqNSTS2/STS37* lines and EV grapevine at 7 dpi. (n) Histochemical staining of RNAi*VqNSTS2/STS37* lines and EV grapevine leaves at 7 dpi stained with trypan blue. Bars = 100 μm. (o) Quantification of spores per mg fresh leaves from RNAi*VqNSTS2/STS37* lines and EV grapevine at 7 dpi. (p) qRT-PCR analysis of resistance-related genes in RNAi*VqNSTS2/STS37* lines and EV grapevine after *E. necator* inoculation. Asterisks indicate significant differences (*$P < 0.05$, **$P < 0.01$, Student's *t* test).

combined with the Pro35S-VqERF062 vector for co-infiltration into tobacco leaves. The co-expression of *VqERF062* and *VqNSTS2* exhibited significantly higher luminescence signals and LUC/REN ratio than the controls did, indicating that VqERF062 positively regulates the expression of *VqNSTS2* (Figure 4a). The above results prompted us to identify the binding sites of VqERF062 on *VqNSTS2* promoter. Previous research showed that AP2/ERF recognize the motifs of GCC-box (GCCGCC), DRE (ACCCAC) and RAA (CAACA) (Cai *et al.*, 2014; Ma *et al.*, 2017; Wang *et al.*, 2019). However, the GCC-box was not found in *VqNSTS2* promoter, but DRE and RAA motifs were found (Figure 4b). Therefore, yeast one-hybrid (Y1H) assays and electrophoretic mobility shift (EMSA) assays were carried out to determine the specific binding motif. As shown in Figure 4b–e, VqERF062 could bind to DRE and RAA motifs in the promoter of *VqNSTS2*.

To further investigate whether *VqERF062* can influence the expression of *VqNSTS2* and stilbene accumulation, the transient overexpression assay was performed in 'Danfeng-2' leaves. Immunoblotting analysis indicated that the band of the VqERF062-GFP fusion proteins were detected in two groups of leaves overexpressing *VqERF062* (Figure 4f). The much higher transcript abundances of *VqERF062* and *VqNSTS2* were detected in two groups of leaves overexpressing *VqERF062* (Figure 4g). HPLC analysis showed that the content of stilbenes increased in both two groups of leaves overexpressing *VqERF062*, especially the content of piceid, which was 1.4 times that of WT (Figure 4h). The above results indicated that VqERF062 could directly bind to *VqNSTS2* promoter resulted in the accumulation of more stilbenes.

VqERF062 enhance resistance to *E. necator* and also activation of resistance-related genes in grapevine

To evaluate the role of *VqERF062* in the resistance to PM, we created *35S-VqERF062-GFP* overexpression plants and *VvERF062*-RNAi plants using pro-embryogenic masses derived
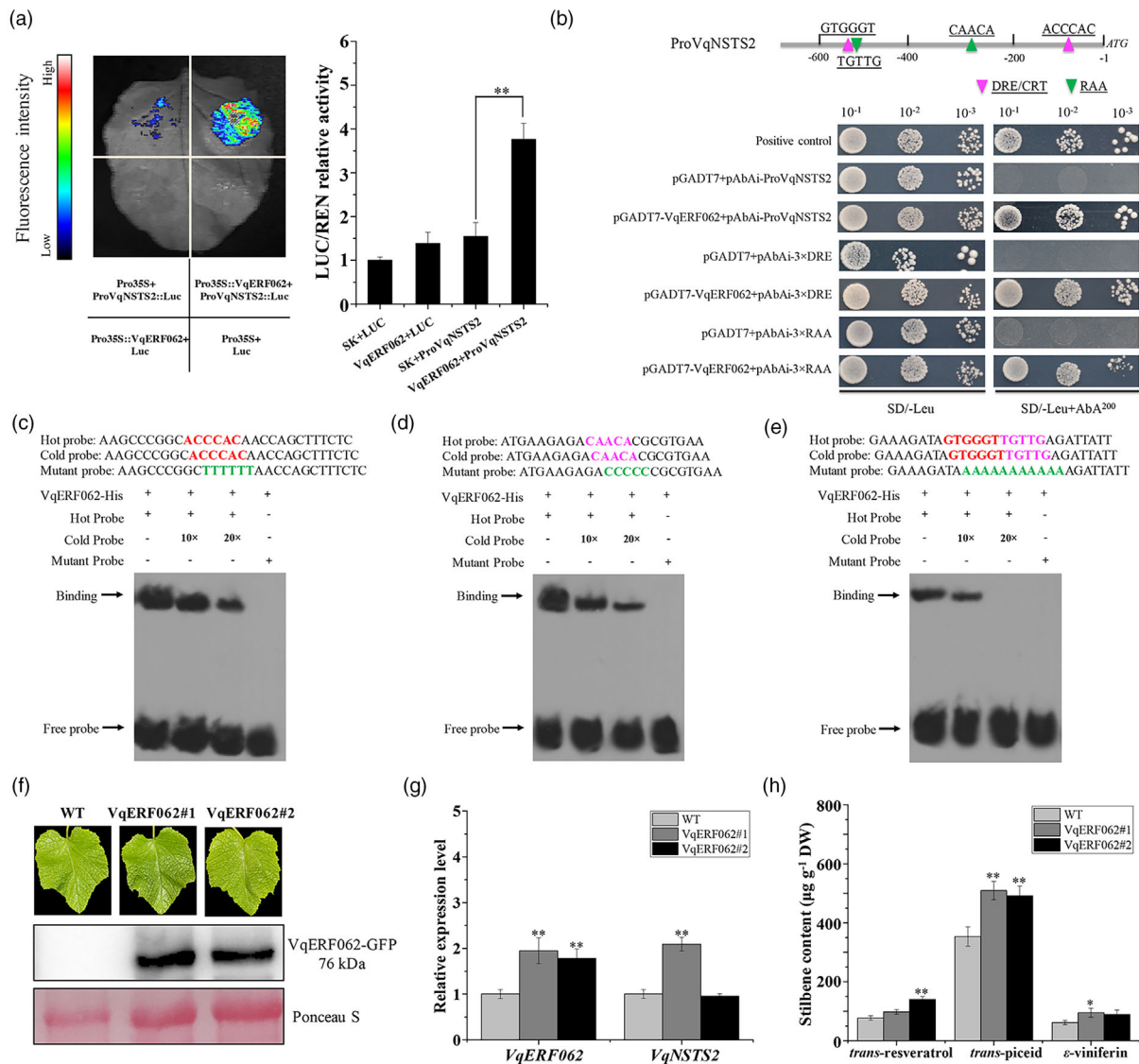
Figure 4 VqERF062 promotes the expression of *VqNSTS2* by binding to its promoter. (a) *ProVqSTS2*-Luc and *Pro35S-VqERF062* were co-infiltrated into tobacco leaves to detect the LUC/RNE ratio. The combinations of Luc and *Pro35S*, Luc and *Pro35S-VqERF062* and *ProVqSTS2*-Luc and Pro35S were co-injected as the controls. (b) Yeast one-hybrid (Y1H) assays showing that VqERF062 binds to DRE and RAA elements in the *VqNSTS2* promoter. p53-pAbAi co-transformed with pGADT7-p53 was used as the positive control. (c–e) Electrophoretic mobility shift assay (EMSA) analysis revealing VqERF062 binding to DRE and RAA elements in the *VqNSTS2* promoter. The VqERF062-His protein was incubated with the biotin-labelled hot probe (ACCCAC and CAACA) or mutant probe (TTTTTT, CCCCC and AAAAAAAAAA), along with or without 10-fold and 20-fold excess of unlabelled cold probe as a competitor. The shifted probes and free DNA probes are indicated by black arrows. −, absence; +, presence. (f) Western blot detection for VqERF062-GFP in transient overexpression and wild type Danfeng-2 leaves. (g) qRT-PCR analyse the expression of *VqERF062* and *VqNSTS2* in transient overexpression and wild type 'Danfeng-2' leaves. (h) Stilbenes contents in the leaves of transient overexpression and wild type Danfeng-2 leaves. One-way ANOVA (Tukey's test) was performed and asterisks indicate significant differences at *$P < 0.05$, **$P < 0.01$.

from 'Thompson Seedless' (Figure 5a–f). Intriguingly, qRT-PCR showed that the expression levels of *PAL* and *CHS* in OE lines and RNAi lines all increased significantly, but *STS* was up-regulated expression in OE lines and down-regulated expression in RNAi lines (Figure 5g,h). Additionally, stilbenes content was significantly increased in OE lines, but almost unchanged in RNAi lines (Figure 5m and Table 3).

To validate the function of VqERF062 in the resistance to PM, the OE lines, RNAi lines and WT were inoculated with PM. Compared with WT, there were fewer fungal spores colonies were observed in the leaves of OE lines, but more in that of RNAi

lines at 7 dpi (Figure 5i). Trypan blue and DAB staining, scanning electron micrographs and quantification of the number of spores revealed the slower hypha growth, more H_2O_2 and HR-like cell death in the leaves of OE lines, but RNAi lines were the opposite (Figure 5j–l). HPLC results showed that the stilbenes content in the OE lines increased more times than that in WT (Figure 5n and Table 3). Compared to WT, qRT-PCR results showed that resistance-related genes exhibited higher transcript levels in OE lines, but not in RNAi lines (Figure 5o–r). These results indicated that *VqERF062* is a positive regulator in response to *E. necator* in grapevine.
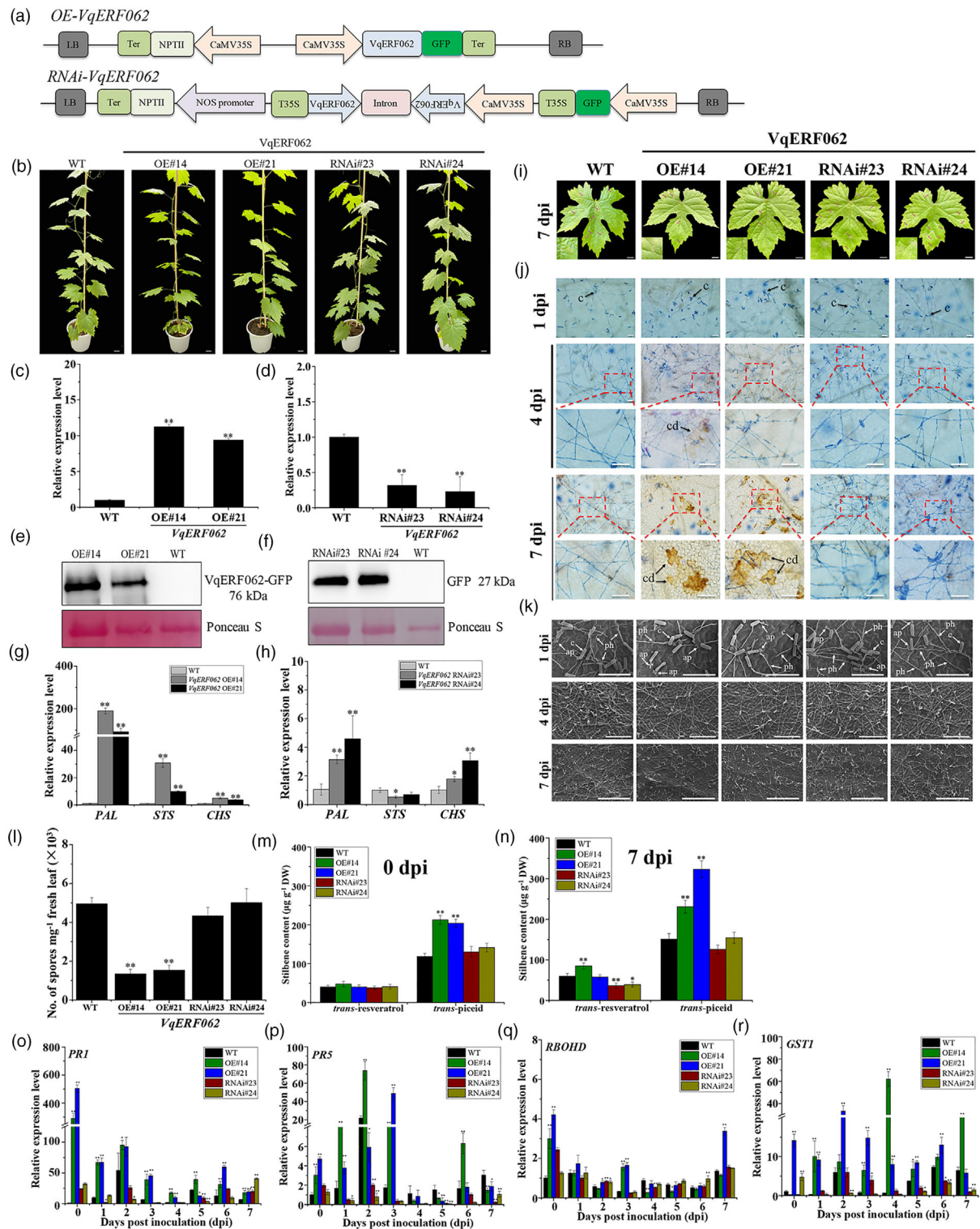
Figure 5 *VqERF062* enhanced resistance to *Erysiphe necator* in grapevine. (a) Schematic diagram of overexpression and RNAi vectors. (b) Photograph of plants showed transgenic plants and WT, Bars = 2 cm. (c, d) Relative transcript levels of *VqERF062* in OE and RNAi plants. (e, f) Western blot detection for VqERF062-GFP (76.5 KDa) in OE and RNAi plants. (g, h) The relative transcript levels of phenylalanine pathway-associated genes in OE and RNAi plants. (i) Leaves showed OE and RNAi plants at 7 dpi. Bar = 1 cm. (j) Histochemical staining of leaves of OE and RNAi plants at 1, 4 and 7 dpi stained with trypan blue and DAB. Bar = 50 μm. (k) Scanning electron micrographs of the hyphae of *E. necator* in OE and RNAi plants. Upper figures bars = 100 μm, middle figures bars = 200 μm and lower figures bars = 500 μm. (l) Quantification of spores per mg fresh leaves from OE and RNAi plants at 7 dpi. One-way ANOVA (Tukey's test) was performed and asterisks indicate significant differences at *$P < 0.05$, **$P < 0.01$. (m, n) Stilbenes content in the leaves of OE and RNAi plants at 0 dpi and 7 dpi. (o–r) qRT-PCR analysis of resistance-related genes in OE and RNAi plants. One-way ANOVA (Tukey's test) was performed and asterisks indicate significant differences at *$P < 0.05$, **$P < 0.01$.

Table 3 Content of stilbenes of *VqERF062* transgenic mutants under natural conditions and after artificial inoculation with *Erysiphe necator* by HPLC

Lines	*Trans*-resveratrol (μg/g)	*Trans*-piceid (μg/g)
WT	40.28 ± 4.37	118.45 ± 8.30
OEVqERF062 OE#14	47.9 ± 6.91	212.79 ± 11.24
OEVqERF062 OE#21	40.34 ± 5.09	204.31 ± 10.08
OEVqERF062 RNAi#23	38.27 ± 4.16	130.35 ± 14.01
OEVqERF062 RNAi#24	40.95 ± 6.22	141.53 ± 10.99
WT-7 dpi	59.94 ± 6.73	151.09 ± 13.59
OEVqERF062 OE#14–7 dpi	85.09 ± 7.34	230.98 ± 15.54
OEVqERF062 OE#21–7 dpi	57.71 ± 5.93	323.12 ± 20.81
OEVqERF062 RNAi#23–7 dpi	36.69 ± 6.19	125.79 ± 10.30
OEVqERF062 RNAi#24–7 dpi	39.12 ± 6.02	154.45 ± 13.76

The interaction of VqERF062 with VqERF1B promotes the expression of *VqNSTS2* enhanced resistance to *E. necator*

To further understand the molecular network of *VqERF062*, we predicted its interacting proteins using the online analysis tool VTCdb (Table S3). The truncated VqERF062$^{\Delta355-442}$ that contained the AP2 domain and lacked self-activation activity was used to further screen the interacting proteins of VqERF062 (Figure S5). Yeast two-hybrid (Y2H) showed that an ERF transcription factor, ERF1B (VIT_05s0049g00510), interacted with VqERF062 in yeast (Figure 6a). Subsequently, the bimolecular fluorescence complementation (BiFC) experiment was used to verify the interaction between VqERF062 and VqERF1B, and YFP fluorescence was detected in the combinations of VqERF062-CE/VqERF1B-NE and VqERF062-NE/VqERF1B-CE, but not in the control combination (Figure 6b). Also, pull-down assays showed that recombinant protein VqERF1B-His was bond by VqERF062-GST but not GST (Figure 6c). Furthermore, the fluorescence resonance energy transfer-acceptor photobleaching (FRET-AB) analysis was confirmed the interaction between VqERF062 and VqERF1B (Figure 6d). As shown in Figure 6e, there were no FRET occurred between GFP and mCherry combination, yielding only background levels of FRET efficiency (2%). In contrast to the control, VqERF062-GFP and VqERF1B-mCherry combination yielded substantially high levels of FRET efficiency, reaching approximately 32% on average. Taken together, these results verified that VqERF062 interacts with VqERF1B *in vivo* and *in vitro*. To further investigate the function of protein complex, VqERF062 and VqERF1B, in *VqNSTS2* expression and stilbene accumulation, dual-luciferase assays was carried out. As shown in Figure 6f, transient overexpression of *VqERF062* activated *VqNSTS2* promoter. The co-overexpression of *VqERF062* and *VqERF1B* induced higher promoter activity of *VqNSTS2* compared with the overexpression of *VqERF062* alone. The above results indicate that the interaction between VqERF062 and VqERF1B promoted the expression of *VqNSTS2*. In addition, we were excited to discover that VqERF062 can interact with itself to form homodimers and exert regulatory functions (Figure S6).

To further explore the regulation mechanism between VqERF062 with VqERF1B, the promoter of *VqERF1B* was cloned. Fortunately, the ERF transcription factor binding site, GCC-box, was found in *VqERF1B* promoter (Figure 6g). Y1H and EMSA assays confirmed the binding of VqERF062 to the promoter of

VqERF1B and revealed that the binding site was GCC-box (Figure 6g,h). To verify that VqERF062 activates the expression of *VqERF1B*, the fusion vectors, ProVqERF1B-Luc and Pro35S-VqERF062, were co-infiltration into tobacco leave. Luc and Pro35S, Luc and Pro35S-VqERF062 and ProVqERF1B-Luc and Pro35S were as the controls. As shown in Figure 6i, higher luminescence signals were observed in the co-expression of ProVqERF1B-Luc and Pro35S-VqERF062 than the controls. In addition, LUC/REN rates were calculated by the dual-luciferase assays. As a result, we found that the LUC/REN relative activity of co-expression of ProVqERF1B-Luc and Pro35S-VqERF062 was significantly higher than the controls (Figure 6j). These results demonstrated that VqERF062 binds specifically to the GCC-box within the promoter of *VqERF1B* and promotes its expression.

VqERF1B is also a positive regulator of enhancing resistance to *E. necator* in grapevine

To explore the function of *VqERF1B*, we first constructed the overexpression and RNA interference vectors (Figure 7a). Subsequently, a transient overexpression and interference assay was carried out in 'Danfeng-2' leaves using *Agrobacterium*-mediated infiltration (Figure 7b). As shown in Figure 7c, the transcript level of *VqERF1B* was more elevated in OE*VqERF1B* leaves than in those containing OE empty vector (OE-EV), with 2.3-fold higher expression. However, the transcript level of *VqERF1B* in RNAi*VqERF1B* leaves was 50% lower than that in RNAi empty vector (RNAi-EV). Consistent with the expression of *VqERF1B*, the content of stilbenes was increased in OE*VqERF1B* leaves and decreased in RNAi*VqERF1B* leaves (Figure 7d and Table 4). Furthermore, we performed trypan blue staining on OE*VqERF1B* leaves and RNAi*VqERF1B* leaves after inoculated with *E. necator*. As shown in Figure 7b, while many whitish mildew colonies were seen on the infected RNAi*VqERF1B* leaves, only scattered and sparse mildew colonies were observed on OE*VqERF1B* leaves at 7 dpi. Trypan blue staining and quantification of the number of spores showed that hyphal growth and sporulation were significantly restricted in OE*VqERF1B* leaves (Figure 7e,f). These results suggested that *VqERF1B* enhance the resistance to PM in grapevine.

Discussion

Specific expression of *VqNSTS2* in the model plant *A. thaliana* and its resistance to *G. cichoracearum* showed an immune response

After powdery mildew infects the plant, it forms haustorium at the invasion site, and the production of haustorium is also the manifestation of the successful colonization of the fungus on the plant (Micali *et al.*, 2008). Haustorium mainly absorbs nutrients and water from plants, while releasing effector factors to inhibit plant immunity. In order to resist the infection of powdery mildew, plants wrap haustorium to form the extra-haustorial matrix (EHMx) (Koh *et al.*, 2005; Meyer *et al.*, 2009; Micali *et al.*, 2011). After the invasion of pathogen, plants can prevent the invasion of pathogenic bacteria by guiding membrane trafficking to form papillae, which is a large amount of callose and other antibacterial substances deposited in the extracellular space between the plasma membrane and the cell wall (Lipka *et al.*, 2008; Wen *et al.*, 2011). After the fungus successfully penetrates the epidermal cells, the host cell forms a second post-invasion defence barrier called the haustorial encasement. The haustorial encasement is a structure that
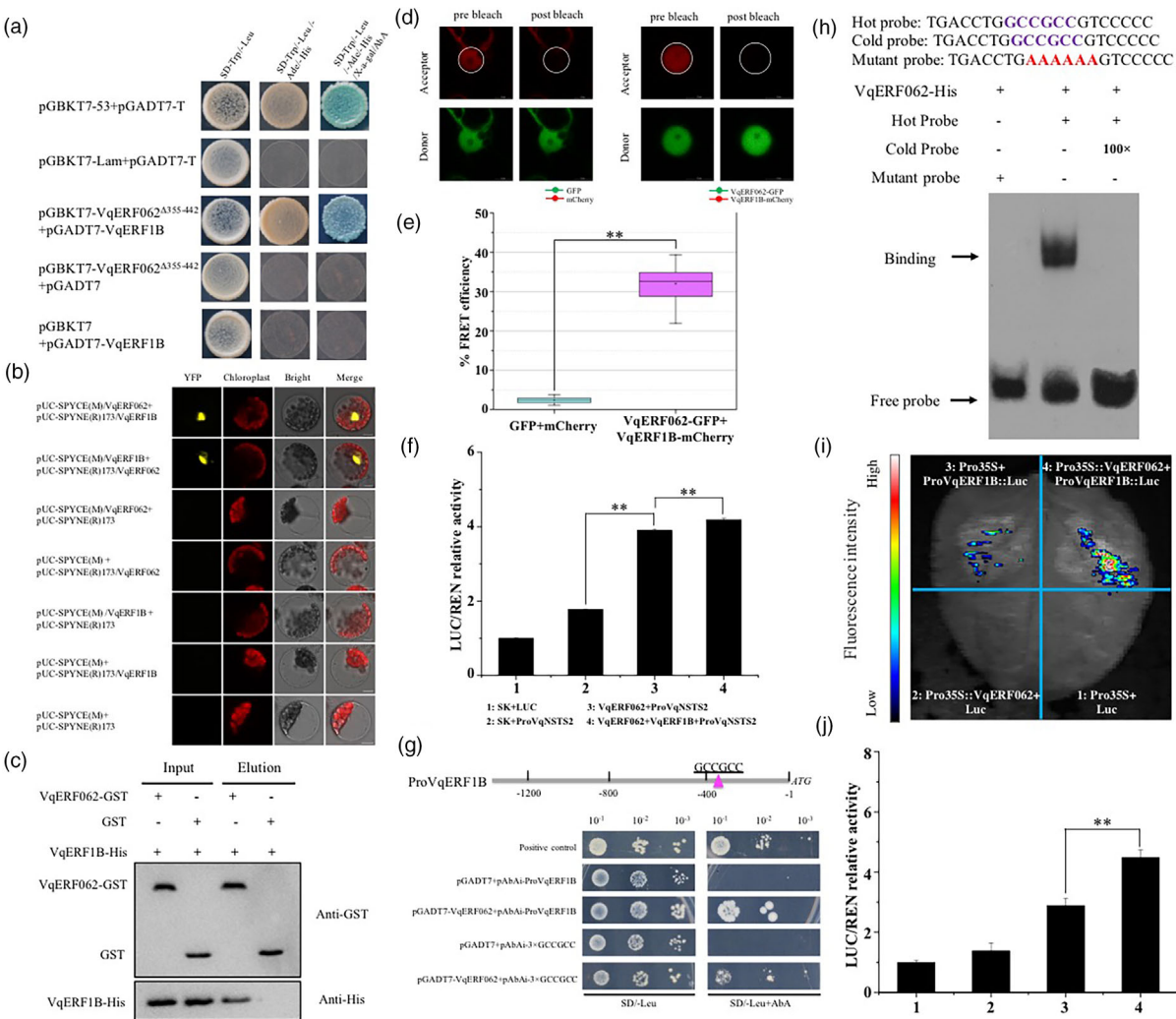
Figure 6 VqERF062 interacts with VqERF1B, which promotes the expression of *VqNSTS2*. (a) Yeast two-hybrid assay. pGBKT7 or pGADT7 plasmid containing VqERF062$^{\Delta355–442}$ and VqERF1B were transformed into Y2HGold. pGADT7-T/pGBKT7-Lam, negative control; pGADT7-T/pGBKT7-53, positive control. (b) Bimolecular fluorescence complementation (BiFC) assays showing that VqERF062 interact with VqERF1B in mesophyll protoplast of Arabidopsis. YFP: yellow fluorescent. Chloroplast: chloroplast auto-fluorescence. Bar = 10 μm. (c) Pull-down assay. The presence or absence of each protein in the mixture is indicated as + or −, respectively. (d, e) Fluorescence resonance energy transfer (FRET) results showing that VqERF062 interact with VqERF1B. Asterisks indicate significant differences (**$P < 0.01$, Student's *t* test). (f) VqERF062-VqERF1B complex enhances the activations to *VqNSTS2* in dual-luciferase assays. The empty vector represented the co-expression of 62-SK and 0800-LUC and the LUC/REN value was set as 1, as a calibrator. One-way ANOVA (Tukey's test) was performed and asterisks indicate significant differences at **$P < 0.01$. (g) Y1H assays showing that VqERF062 binds to the promoter of VqERF1B and GCC-box. The positive control is pGADT7-p53 + p53-pAbAi. (h) Electrophoretic mobility shift assay (EMSA) analysis revealing VqERF062 binding to GCCGCC element in the VqERF1B promoter. The VqERF062-His protein was incubated with the biotin-labelled hot probe (GCCGCC) or mutant probe (AAAAAA), along with or without a 100-fold excess of unlabelled cold probe as a competitor. The shifted probes and free DNA probes are indicated by black arrows. −, absence; +, presence. (i) Images of tobacco leaves 3 days after co-infiltration. proVqERF1B-Luc and pro35S-VqERF062 were co-infiltrated into tobacco leaves to detect the LUC/RNE ratio. The combinations of Luc and pro35S, Luc and pro35S-VqERF062 and proVqERF1B-Luc and pro35S were co-injected as the controls. (j) The LUC/RNE relative activity assays for VqERF062 activation of the *VqERF1B* promoter. The value for luminescence intensity of Luc and Pro35S was set to 1. 1: Pro35S + Luc; 2: Pro35S::VqERF062 + Luc; 3: Pro35S + ProVqERF1B::Luc; 4: Pro35S::VqERF062 + ProVqERF1B::Luc. One-way ANOVA (Tukey's test) was performed and asterisks indicate significant differences at **$P < 0.01$.

extends from the papillae and isolates the haustorium from the host cells, thus limiting fungal proliferation by preventing the absorption of nutrients. The haustorial encasement is rich in callose, phytoalexin and other antibacterial components (Rubiato et al., 2022). Many previous studies have shown that *STS* genes in grapes are located in different positions at different stages of plant growth and development. After transforming VpSTS29-GFP into grape protoplasts, it was observed that green fluorescence was mainly located in cytoplasm and endoplasmic reticulum through laser scanning confocal microscopy. At the same time, VpSTS29-GFP is also present in the tiny organelle – the oil body and can be transported to the vacuole at a specific stage of plant development (Ma et al., 2018; Xu et al. 2019b). In grape berries, STSs exist in the exocarp of the berry at various stages of fruit
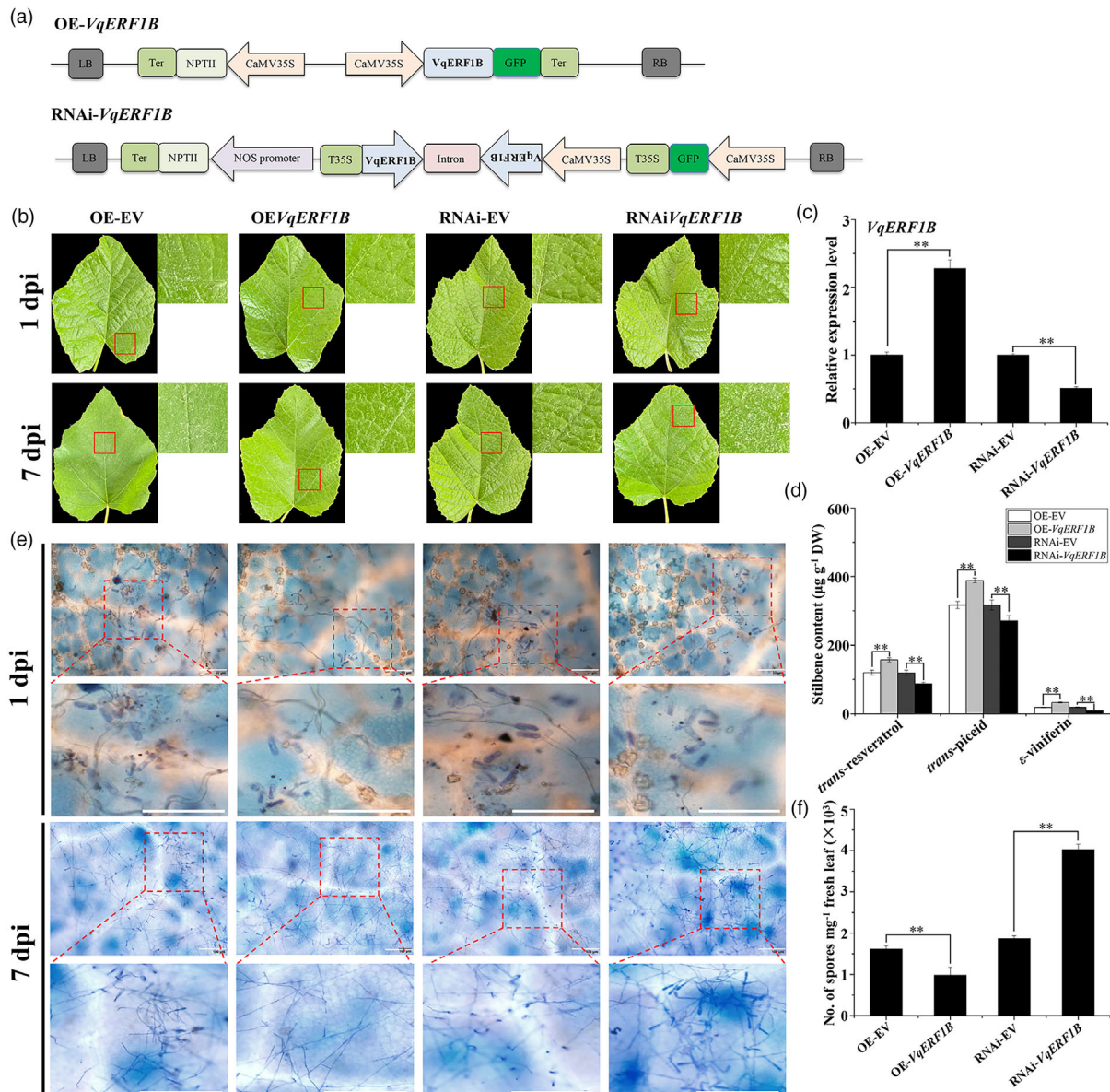
Figure 7 *VqERF1B* is a positive regulator of powdery mildew resistance in grapevine. (a) Schematic diagram of OE and RNAi vectors. (b) Photograph of leaves of OE*VqERF1B* lines, RNAi*VqERF1B* lines and EV grapevine. dpi, days post inoculated with *E. necator*. (c) The transcription level of *VqERF1B* in OE*VqERF1B* lines, RNAi*VqERF1B* lines and EV grapevine at 0 dpi. (d) Stilbenes contents in the leaves of OE*VqERF1B* lines, RNAi*VqERF1B* lines and EV grapevine leaves at 0 dpi. One-way ANOVA (Tukey's test) was performed and asterisks indicate significant differences at $**P < 0.01$. (e) Histochemical staining of OE*VqERF1B* lines, RNAi*VqERF1B* lines and EV grapevine leaves at 7 dpi stained with trypan blue. Bars = 100 μm. (f) Quantification of spores per mg fresh leaves from OE*VqERF1B* lines, RNAi*VqERF1B* lines and EV grapevine at 7 dpi.

Table 4 Content of stilbenes in grapevine leaves transiently expressing the transcription factor *VqERF1B* by HPLC analysis

Lines	*Trans*-resveratrol (μg/g)	*Trans*-piceid (μg/g)	ε-viniferin (μg/g)
OE-EV	120.18 ± 7.20	317.12 ± 10.76	18.67 ± 0.65
OE*VqERF1B*	157.41 ± 5.89	389.00 ± 7.10	33.05 ± 1.85
RNAi-EV	119.53 ± 7.26	317.11 ± 14.89	18.97 ± 1.31
RNAi*VqERF1B*	87.98 ± 4.07	271.24 ± 15.01	8.79 ± 0.41

development (Fornara *et al.*, 2008). Pan's study found that STS was mainly located on the cell wall, secondary cell wall and chloroplast during the development of berries (Pan *et al.*, 2009). To figure out where VqNSTS2 positioned when it interacts with powdery mildew, we transferred VqNSTS2 with its own promoter in *A. thaliana, which* was *STS* absent and inoculated the plants with *G. cichoracearum* (Figure 2). It was found that with the spore germination the green fluorescence of VqNSTS2 was gathered at the invasion site of *G. cichoracearum* (Figure 2). And with the invasion time increased the haustorium was totally sealed by VqNSTS2-GFP and formed the haustorial encasements

to prevent the invasion of fungus and play a disease-resistant immune response. To sum up, VqNSTS2-GFP actively accumulated at the infection sites of *G. cichoracearum* and then wrapped the haustorium to form the encasement to prevent the invasion of *G. cichoracearum* in *A. thaliana*.

Role of *VqNSTS2* in metabolic pathway and its resistance to powdery mildew

Stilbenes exhibit broad-spectrum resistance to a variety of pathogens (Hain *et al.*, 1993; Khattab *et al.*, 2021; Pezet *et al.*, 2004; Xu *et al.*, 2019a). A large number of studies have proved that transforming *STS* into various plants can improve the disease resistance of transgenic plants by producing stilbenes. The first report of increased disease resistance in *STS* transgenic plants was conducted by Hain *et al.* (1993). They transferred a *VvSTS* into tobacco resulted in the more resistant to *B. cinerea*. Subsequently, this team stably integrated *VvSTS* into the tomato genome and the transgenic tomato exhibited significant increase in the resistance to *Phytophthora infestans* (Thomzik *et al.*, 1997). It has been reported that *VvSTS* transgenic rice, barley or papaya can increase resistance to *P. oryzae*, *B. cinerea* or *P. palmivora*, respectively (Leckband and Lörz, 1998; Stark-Lorenzen *et al.*, 1997; Zhu *et al.*, 2004). There are also many reports on the function of *STSs* in Chinese wild grape germplasm resources. *VpSTSgDNA2* cloned from Chinese wild *V. pseudoreticulata* accession 'Baihe-35-1' was transferred in *V. vinifera* L. cv. 'Chardonnay', resulting in increased resistance to PM, manifested more stilbenes and H_2O_2 and the reduced growth of PM (Dai *et al.*, 2015). The heterologous overexpression of *VqSTS21* or *VqSTS36* cloned from Chinese wild *V. quinquangularis* accession 'Shang-24' in Arabidopsis increased the resistance to PM (Huang *et al.*, 2016, 2018). *VqSTS6*, from Chinese wild *V. quinquangularis* accession 'Danfeng-2', increases the content of stilbenes and the resistance to PM of transgenic plants of 'Thompson Seedless' (Cheng *et al.*, 2016). In our study, *VqNSTS2*, a novel *STS* isolated from 'Danfeng-2', significantly increased the resistance to PM in transgenic 'Thompson Seedless' by activating immune signalling pathways, including the production of more stilbenes, callose deposition and H_2O_2 (Figure 3). However, unlike previous reports (Liu *et al.*, 2019), PM-resistant plants overexpressing *VqNSTS2* exhibited HR-like cell death, a typical symptom of ETI (Figure 3d).

SA and JA are the most studied defence pathways, which form the backbone of the hormone-regulated part of the immune system (Aerts *et al.*, 2021). In this study, SA and JA signalling-related genes were activated in responding to PM in *35S-VqNSTS2-GFP* overexpression plants (Figure 3i). Likewise, the overexpression of *VpSTS29/STS2* from 'Baihe-35-1' increased resistance to PM in *V. vinifera* L. cv. 'Thompson Seedless' and Arabidopsis by producing more stilbenes and activating SA signalling (Xu *et al.*, 2019a). Therefore, we speculated that *STS* function as the positive regulator against to PM by activating multiple signalling pathway.

The complex mechanism of transcriptional cascade VqERF062-VqERF1B regulation and its enhanced resistance to powdery mildew

The AP2/ERF TFs family play key roles in regulating biosynthesis of primary and secondary metabolism. For example, CitERF71 directly bound to ACCCGCC and GGCGGG motifs in the promoter of *CitTPS16* resulted in production of *E*-geraniol in *Citrus* fruit (Li *et al.*, 2017). ORCA3 and ORCA4 played key roles in the biosynthesis of terpenoid indole alkaloids in *Catharanthus*

roseus (Paul *et al.*, 2017). NaERF1B-like transcription factor, as a key node, plays an important role in plant defence against *Alternaria alternate* by integrating various signals such as plant hormones and WRKY-type transcription factors to regulate the synthesis of phytoalexins scopoletin and solavetivone (Ma *et al.*, 2024). In *Isatis indigotica*, the AP2/ERF, Ii049, bound to the CE1, RAA and CBF2 motifs of key structural genes, *IiPAL* and *IiCCR*, in the lignan/lignin pathway (Ma *et al.*, 2017). SmERF73 and SmERF128 enhanced tanshinone accumulation by binding to GCC-box, CBF2 and RAA motifs on the promoters of tanshinone-associated genes such as *DXR1*, *CPS1*, *KSL1*, *CYP76AH1* and *CYP76AH3* (Zhang *et al.*, 2019; Zheng *et al.*, 2021). The MdERF109 protein promoted coloration by directly binding to GCC-box on the promoters of anthocyanin-related genes, including *MdCHS*, *MdUFGT* and *MdbHLH3* (Ma *et al.*, 2021). Another AP2/ERF, MdAP2-34, promoted carotenoid accumulation by binding to ACCGAC motif in the *MdPSY2-1* promoter (Dang *et al.*, 2021). CsERF061 recognized ERE motif or GCC-box on the promoters of nine key carotenoid pathway genes (*PSY1*, *PDS*, *CRTISO*, *LCYb1*, *BCH*, *ZEP*, *NCED3*, *CCD1* and *CCD4*) and enhanced carotenoid accumulation (Zhu *et al.*, 2021). Stilbenes is kind of phenolic secondary metabolism existed in many plant. In this study, VqERF062 could regulate the expression of *VqNSTS2* by directly binding DRE and RAA motifs resulted in the accumulation of stilbenes (Figure 4). This is consistent with a previous study of *Artemisia annua TAR1*, which reported that AP2/ERF could control the accumulation of artemisinin by recognizing GCC-box, CBF2 (GTCGAC) and RAA (CAACA) motifs to regulate two enzyme genes, *CYP71AV1* and *ADS*, in the biosynthesis of artemisinin (Tan *et al.*, 2015). There were reports indicated that AP2/ERF also involved in the biosynthesis of other kinds of metabolites, such as camptothecin (Hu *et al.*, 2020), capsaicinoid (Song *et al.*, 2020), notoginsenoside (Lin *et al.*, 2020) and gypenoside (Xu *et al.*, 2020).

AP2/ERF paly vital roles in the defence to biotic stresses, and many reports have revealed that ERF from several species enhance the immunity against fungal and bacterial diseases. A tomato ERF, ERF68, positively regulated HR-like cell death and *Xanthomonas* spp. by activating multiple signalling pathways including ET, SA and JA (Liu and Cheng, 2017). *ZmERF105* enhanced the defence against *Exserohilum turcicum* by prompting the expression of five pathogenesis-related (*PR*) genes (Zang *et al.*, 2020). ZmERF061 involved in the resistance to *E. turcicum* by regulating the expression of *PRs*, SA- and JA-related genes (Zang *et al.*, 2021). MdERF11 was found to act as a positive regulator against *Botryosphaeria dothidea* by increasing SA synthesis (Wang *et al.*, 2020b). CmERF27 regulates red light-induced ethylene biosynthesis to resist *Podosphaera xanthii* infection, which is the agent of PM in melons (Wu *et al.*, 2024). In the present study, VqERF062 could enhance the resistance to PM by activating multiple signalling pathways including SA and JA, and promoting HR-like cell death and callose deposition (Figure 5). Similarly, VaERF20 elevated resistance to *B. cinerea* and *Pseudomonas syringae* by increasing the expression of PTI genes and SA- and JA-related genes, and the accumulation of callose and reactive oxygen species (ROS) (Wang *et al.*, 2018). These results are consistent with the previous studies demonstrating that ERFs act as positive regulators against various diseases (Hong *et al.*, 2022; Pillai *et al.*, 2020). However, there were also several reports demonstrated that ERF transcription factors were the negative regulator against diseases. For example, AtERF19 negatively regulated the resistance to *B. cinerea*,
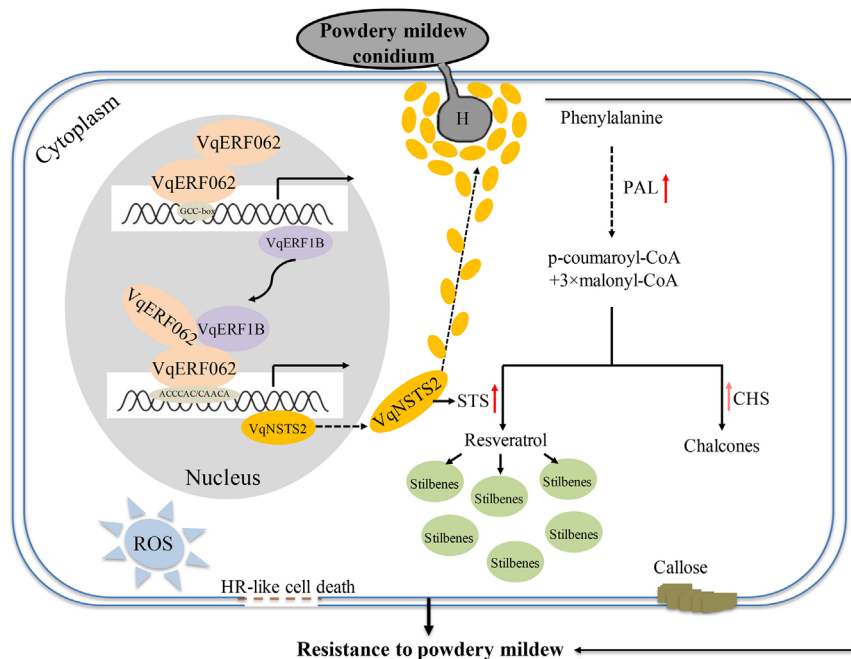
Figure 8 Proposed model of *VqNSTS2* in the phenylalanine metabolism pathway in participating in powdery mildew resistance. When plants are exposed to powdery mildew, *VqNSTS2* was activated rapidly and wrapped the haustorium of spores to inhibit the invading of powdery mildew. Further, the overexpression of *VqNSTS2* enhance resistance to powdery mildew by promoting the accumulation of stilbenes, H_2O_2, callose and HR-like cell death and the expression of resistance-related genes. Besides, VqERF062, in the form of a complex, VqERF062-VqERF1B, activates the expression of *VqNSTS2* via directly bind to DRE and RAA motifs on the *VqNSTS2* promoter.

Pseudomonas syringae and *Phytophthora parasitica* by repressed MAMP-induced PTI outputs (Huang *et al.*, 2019; Lu *et al.*, 2020). Overexpressing GmAP2 transgenic soybean hairy roots exhibited hypersensitivity to *Phytophthora sojae*, whereas roots of GmAP2-RNAi transgenic soybean exhibited enhanced resistance (Zhang *et al.*, 2021).

TFs bind to DNA and control the expression of corresponding genes in the form of single protein or protein complexes formed by physical interaction with other TFs (Bemer *et al.*, 2017). In this study, VqERF062 formed protein complexes by physical interaction with VqERF1B, which enhanced the regulation to *VqNSTS2* (Figure 6). This is consistent with a previous study, CitERF32 and CitERF33 activated the transcription of *CitCHIL1*, while CitRAV1 formed a transcription complex with CitERF33 that strongly enhanced the activation efficiency and flavonoid accumulation (Zhao *et al.*, 2021). However, this protein–protein interaction sometimes also weakens the regulatory role of one or the other. For example, MdERF2 and MdERF3 proteins directly interact and this interaction suppresses the binding of MdERF3 to the MdACS1 promoter (Li *et al.*, 2016). Furthermore, VqERF062 could directly bind to GCC-box on the promoter of *VqERF1B* promoting the expression of *VqERF1B* (Figure 6G–J). Therefore, we demonstrated that VqERF062 and VqERF1B protein complexes participated in the transcriptional regulation of *VqNSTS2* in a positive feedback loop.

In conclusion, the results demonstrated and characterized the new STS family member, *VqNSTS2*, from 'Danfeng-2' based on our previous research. VqNSTS2 actively accumulated at the invasion sites of *G. cichoracearum* and then wrapped the haustorium of spores to form the physical barrier and prevented them from invading the plants showed an immune response. Furthermore, we observed that *VqNSTS2* enhanced

resistance to PM not only by producing a large amount of stilbenes, H_2O_2, callose deposition and HR-like cell death, but also by promoting the expression of resistance-related genes. In addition, VqERF062, in the form of a complex, VqERF062-VqERF1B, directly banded to DRE and RAA motifs on the *VqNSTS2* promoter to promote the expression of *VqNSTS2* (Figure 8). The results of this study provide insights that will aid future studies of the mechanisms underlying the STS-mediated powdery mildew response as well as grape disease resistance breeding.

Experimental procedure

Plant materials and growth conditions

The Chinese wild grapevines *V. quinquangularis* accession 'Danfeng-2' was cultivated in the Grape Germplasm Resource Nursery of Northwest A&F University, Yangling, Shaanxi, China. Tobacco plants (*Nicotiana benthamiana*) used for dual-luciferase assays and FRET-AB assays were grown in the phytotron (25 °C; photoperiod 16/8 h). *A. thaliana* ecotype Col-0 used for subcellular localization, BiFC and function analysis were grown in a chamber at 23 °C under a light/dark cycle of 16/8 h. The pro-embryogenic masses of 'Thompson Seedless' used for generation of transgenic grapevine were cultured on X6 medium (4.43 g/L MS, 60 g/L sucrose, 3 g/L phytagel, 1.5 g/L activated carbon, PH: 5.8–6.2) in darkness at 25 °C (Zhou *et al.*, 2014).

Gene cloning and sequence analysis

Full-length coding sequences (CDSs) of *VqNSTS2*, *VqERF062* and *VqERF1B* were cloned from the cDNA of 'Danfeng-2' leaves, and the promoters of *STSs* and *VqERF1B* were obtained from the gDNA of 'Danfeng-2' leaves. Primers were listed in Table S4.

Amino acid sequence alignment was carried out using DNAMAN software (Version 5.2.2, Lynnon Biosoft, USA). The multiple alignment was performed using Clustal X, and the phylogenetic tree was conducted using FigTree v1.4.4.

Generation and detection of transgenic grapevine

To obtain overexpression vector, the CDS of *VqNSTS2*, *VqERF062* and *VqERF1B* without termination codon were separately cloned into pCAMBIA2300-GFP vector to generate the fusion vectors *VqNSTS2-GFP* and *VqERF062-GFP*. In order to generate RNAi vector, a 200-bp fragment of *VqNSTS2* and a 207-bp fragment of *VqERF062* were inserted into pK7GWIWG2 (II) vector, respectively. All recombinant vectors were separately introduced into *Agrobacterium tumefaciens* strain GV3101. Using pro-embryogenic masses of 'Thompson Seedless' as material, *Agrobacterium*-mediated transformation method was adopted to transformation using a previously described method (Zhou *et al.*, 2014). To verify the integration and expression of exogenous fusion genes in transgene plants, Quantitative Real-Time PCR (qRT-PCR) and western blot assays were performed according to the previous report (Xu *et al.*, 2019a). WT plants was the negative control.

RNA extraction and qRT-PCR reactions

Total RNA extraction of samples from grape was performed according to the protocols of Omega Plant RNA Kit (Omega). The concentration and purity of total RNA were detected using NanoDrop One (Thermo Fisher Scientific, USA). The synthesis of the first strand of cDNA was carried out using the FastKing RT Kit (Tiangen, Beijing, China). qRT-PCR were performed using the NovoStart® SYBR qPCR SuperMix Plus (Novoprotein, Shanghai, China) on Applied Biosystems QuantStudio 6 Flex (Thermo Fisher Scientific, USA). Reactions were run under the following amplification program: 95 °C for 1 min, then 95 °C for 20 s, 50–60 °C for 20 s and 72 °C for 30 s, for 45 cycles. Primers were designed with Primer Premier 5 and assessed by the Primer-BLAST online program (https://www.ncbi.nlm.nih.gov/tools/primer-blast/index.cgi?LINK_LOC=BlastHome). The grapevine *Actin* gene (GenBank No. AY680701) and the Arabidopsis *Actin* gene (GenBank No. AT3G18780) were employed as the internal control gene (Table S4). The $2^{-\Delta\Delta c(t)}$ method (Livak and Schmittgen, 2001) was used to calculate relative gene expression levels. Data are means ($\pm$SD) of three biological replicates.

Extraction and determination of stilbenes

Transient overexpressed 'Danfeng-2' leaves and leaves collected from transgenic grapevine lines and WT plants were vacuum freeze-dried for 24 h. Methanol was added according to the dry weight of samples and extracted for 12 h at 4 °C in darkness. Then the extracts were filtered with the 0.22 μm membrane film and collected for High Performance Liquid Chromatography (HPLC) analysis. The determination of stilbenes was performed on liquid chromatography AcQuity® Arc system (Waters, USA) as previously described (Cheng *et al.*, 2016). The different retention times of stilbenes (Sigma-Aldrich, St Louis, MO, USA) were calibrated with standard samples. Stilbenes content was calculated from the average of three biological replicates.

E. necator infection and histochemical staining

E. necator was collected from the leaves of susceptible *V. vinifera* cultivars. The transgenic grapevines and WT plants were inoculated with *E. necator* according to the previously described

(Wang *et al.*, 1995). The numbers of fungal spores were quantified as previously reported (Weßling and Panstruga, 2012). In brief, inoculated leaves were collected at 7 dpi and cut into pieces into 5 mL sterile water containing 0.01% Tween-20. Shaking for 30 min at 500 rpm and then the blood cell counting plate was used for counting the spores numbers using microscope.

Trypan blue and 3,3′-diaminobenzidine (DAB) were conducted to visualize hypha and H_2O_2 accumulation, and NBT staining was used to visualize O_2^- levels (Koch and Slusarenko, 1990; Thordal-Christensen *et al.*, 1997). The H_2O_2 contents were measured using Hydrogen Peroxide Assay Kit (Solarbio) by fluorescence spectrophotometry. All samples were made in triplicate. Aniline blue staining were performed to quantify the PM-induced callose deposition.

Y1H assays

The promoters of *VqNSTS2* and *VqERF1B* were cloned into the pAbAi vector to build pAbAi-*ProVqNSTS2* and pAbAi-*ProVqERF1B*. The three tandem repeats of GCCGCC (GCC-box) was also inserted into pAbAi vector. The pAbAi-baits were integrated separately into the genome of the Y1HGold yeast strain according to the instruction of the Yeastmaker Yeast Transformation System 2 User Manual (Clontech). The minimal inhibitory concentrations of Aureobasidin A (AbA) for the bait strains were confirmed according to the system user manual. The CDS of *VqERF062* was inserted into pGADT7 (AD) (Clontech) to generate the AD-prey vector. AD-VqERF062 was transformed into different bait strains and cultured on the medium SD/Leu/AbA. The positive control is pGADT7-p53 + p53-pAbAi. The primers are listed in Table S4.

ChIP-qPCR

For ChIP-qPCR analysis, 3 g young leaves of *35S-VqERF062-GFP* transgenic plants were crosslinked in 0.5% formaldehyde by vacuum infiltration for 10 min. Chromatin was isolated using the EpiQuik Plant ChIP Kit (Epigentek, Santiago, USA) and immuno-precipitated by anti-GFP. The immunoprecipitated and input DNA samples were used for qPCR analysis. The primers are listed in Table S4. The ChIP-qPCR results are presented as percentages of the input DNA.

EMSA assays

To obtain the purified recombinant protein, CDS of *VqERF062* was cloned into pET-32a (+) vector (Novagen, Madison, WI) and transformed into *Escherichia coli* BL21 (DE3). The VqERF062-His recombinant protein was induced by 0.1 mM *β*-D-thiogalactopyranoside (IPTG) (Solarbio Beijing, China) in *E. coli* and purified by using Ni-tagged protein purification kit (CWBIO). The probes were synthesized by Sangon Biotech Co., Ltd (Shanghai, China) and listed in Table S4. EMSA was performed as previously described (Xie *et al.*, 2018) using a LightShift® Chemiluminescent EMSA Kit (20 148, Thermo Scientific, USA).

Transient Dual-Luciferase assay

The CDS of *TFs* were inserted into pGreen II 62-SK vector to generate the effectors, and the promoters of *VqNSTS2* and *VqERF1B* were cloned into pGreen II 0800-LUC vector to generate the luciferase reporters, respectively. All recombinant vectors were, respectively, transformed into *Agrobacterium* strain GV3101 containing pSoup-p19. The transient expression assays

were performed in tobacco leaves. The strains OD_{600} of different combines were adjusted to 0.4 and infiltrated into tobacco leaves. The leaves were collected 3 days later for capturing the fluorescence images with the living imaging apparatus (Lumazone Pylon 2048B) and assessing the ratio of enzyme activities of Firefly luciferase (LUC) and Renilla luciferase (REN) using the Dual Luciferase Reporter Gene Assay Kit (YEASEN, China). The primers are listed in Table S4.

Subcellular localization analysis

The recombinant vector *VqNSTS2-GFP* and a plasma membrane-localized marker PM-RK-mCherry fusion vector (Nelson *et al.*, 2007) were co-injected into 4-week-old tobacco leaves. In addition, the recombinant vector *VqERF062-GFP* and a nuclear localization marker fusion vector, 35S-AtHY5-mCherry (Yao *et al.*, 2017), were co-transformed into *Arabidopsis* protoplasts *via* polyethylene glycol (PEG) and Ca^{2+}-mediated transformation (Zhao *et al.*, 2016). Empty pCAMBIA2300 was used as control. The tobacco plants and *Arabidopsis* protoplasts were cultured at 25 °C for 72 h and 20 h, respectively. The green fluorescent protein (GFP) signal and mCherry signal were observed under 488 nm and 552 nm, respectively, using the confocal laser scanning microscope (Leica TCS SP8, Germany).

Y2H assays

The full-length or truncated CDS of *VqERF062* were inserted into the vector pGBKT7 (BD) (Clontech, Mountain View, CA, USA), forming BD-VqERF062. The CDS of *VqERF1B* was separately inserted into the vector AD to generate AD-VqERF1B. Primers were listed in Table S4. The fusion plasmid BD-VqERF062 was co-transformed with AD-VqERF1B into the Y2HGold yeast strain (Clontech) according to the instruction of the Yeastmaker Yeast Transformation System 2 User Manual. pGBKT7-53/pGADT7-T and pGBKT7-Lam/pGADT7-T acted as positive control and negative control, respectively. Transformed Y2HGold strains were cultured on the medium SD/-Leu/-Trp and SD/-Trp/-Leu/-Ade/-His containing aureobasidin A (AbA) (200 ng/mL) and X-α-gal (40 μg/mL).

BiFC assays

The CDS sequences of *VqERF062* and *VqERF1B* were subcloned into pSPYNE (R) 173 vector or pSPYCE (M) vector (Waadt *et al.*, 2010). The recombinant vectors were transformed into *Arabidopsis* protoplasts for further analysis *via* PEG and Ca^{2+}-mediated transformation (Zhao *et al.*, 2016). The protoplasts after plasmids transformation were cultured 25 °C for 20 h, and then the yellow fluorescent protein (YFP) signal was observed using a confocal laser scanning microscope (Leica TCS SP8, Germany). Primers were listed in Table S4.

FRET-AB assays

FRET-acceptor photobleaching analysis was conducted according to previously reported (Mehlhorn *et al.*, 2018). The FRET-AB efficiency between VqERF062-GFP with its interaction proteins, VqERF1B-mCherry, was measured in tobacco leaves. Scanned nuclei images for free or fused GFP and mCherry protein were collected under 488 nm and 552 nm. The region of interest (ROI) was photobleached by continuously scanning with the 552 nm laser (mCherry) line at 100% intensity for 6 s. The mean FRET efficiency calculated from three different biological replicates and measurements of up to 6 nuclei each replicate. Primers were listed in Table S4.

Pull-down assays

To obtain the fusion proteins VqERF062-GST and VqERF1B-His, the CDS sequences of *VqERF062* and *VqERF1B* were subcloned into pGEX-4T-1 vector or pET-32a vector. The fusion proteins was induced by IPTG in *E. coli*. VqERF062-GST protein was mixed with VqERF1B-His and the mixture was incubated at 4 °C for 12 h. And then the mixture was purified by using Ni-tagged protein purification kit (CWBIO). The purified proteins were then detected by anti-GST antibody and anti-His antibody.

Author contributions

YW designed the research. CY and WL conducted the experiments; RL identified six new stilbene synthetase genes from 'Danfeng-2'; CY cloned the 6 new *STS* genes, analysed the gene structure and function, transiently transformed the new *STS* genes into tobacco and determined the expression of stilbenes; CY, WL and GL analysed the data and wrote the manuscript; YW reviewed and revised the manuscript.

Acknowledgements

Conflict of interest

The authors declare that there is no conflict of interest.

Data availability statement

The data that supports the findings of this study are available in the supplementary material of this article.

References

Aerts, N., Mendes, M.P. and Wees, S.C.M.V. (2021) Multiple levels of crosstalk in hormone networks regulating plant defense. *Plant J.* **105**(2), 489–504.

Atak, A. (2024) *Vitis* species for stress tolerance/resistance. *Genet. Resour. Crop. Evol.* **72**(2), 2425–2444.

Bemer, M., Dijk, A.D.J.V., Immink, R.G.H. and Angenent, G.C. (2017) Cross-family transcription factor interactions: an additional layer of gene regulation. *Trends Plant Sci.* **22**(1), 66–80.

Cai, X.-T., Xu, P., Zhao, P.-X., Liu, R., Yu, L.-H. and Xiang, C.-B. (2014) Arabidopsis ERF109 mediates cross-talk between jasmonic acid and auxin biosynthesis during lateral root formation. *Nat. Commun.* **5**(5), 5833.

Chen, K., Tang, W., Zhou, Y., Chen, J., Xu, Z., Ma, R., Dong, Y. *et al.* (2022) AP2/ERF transcription factor *GmDREB1* confers drought tolerance in transgenic soybean by interacting with GmERFs. *Plant Physiol. Biochem.* **170**, 287–295.

Cheng, S., Xie, X., Xu, Y., Zhang, C., Wang, X., Zhang, J. and Wang, Y. (2016) Genetic transformation of a fruit-specific, highly expressed stilbene synthase gene from Chinese wild *Vitis quinquangularis*. *Planta* **243**(4), 1041–1053.

Chong, J., Poutaraud, A. and Hugueney, P. (2009) Metabolism and roles of stilbenes in plants. *Plant Sci.* **177**(3), 143–155.

Coutos-Thévenot, P., Poinssot, B., Bonomelli, A., Yean, H., Breda, C., Buffard, D., Esnault, R. *et al.* (2001) In vitro tolerance to *Botrytis cinerea* of grapevine 41B rootstock in transgenic plants expressing the stilbene synthase *Vst1* gene under the control of a pathogen-inducible *PR10* promoter. *J. Exp. Bot.* **52**(358), 901–910.

Dai, L., Zhou, Q., Li, R., Du, Y., He, J., Wang, D., Cheng, S. *et al.* (2015) Establishment of a picloram-induced somatic embryogenesis system in *Vitis*

vinifera cv. chardonnay and genetic transformation of a stilbene synthase gene from wild-growing Vitis species. *Plant Cell Tissue Organ Cult.* **121**(2), 397–412.

Dang, Q., Sha, H., Nie, J., Wang, Y., Yuan, Y. and Jia, D. (2021) An apple (*Malus domestica*) AP2/ERF transcription factor modulates carotenoid accumulation. *Hortic. Res.* **8**(1), 223.

Fang, L., Hou, Y., Wang, L., Xin, H., Wang, N. and Li, S. (2014) Myb14, a direct activator of STS, is associated with resveratrol content variation in berry skin in two grape cultivars. *Plant Cell Rep.* **33**(10), 1629–1640.

Fornara, V., Onelli, E., Sparvoli, F., Rossoni, M., Aina, R., Marino, G. and Citterio, S. (2008) Localization of stilbene synthase in *Vitis vinifera* L. during berry development. *Protoplasma* **233**(1–2), 83–93.

Hain, R., Reif, H.J.R., Krause, E., Langebartels, R., Kindl, H., Vornam, B., Wiese, W. *et al.* (1993) Disease resistance results from foreign phytoalexin expression in a novel plant. *Nature* **361**(6408), 153–156.

Höll, J., Vannozzi, A., Czemmel, S., D'Onofrio, C., Walker, A.R., Rausch, T., Lucchin, M. *et al.* (2013) The R2R3-MYB transcription factors MYB14 and MYB15 regulate stilbene biosynthesis in *Vitis vinifera*. *Plant Cell* **25**(10), 4135–4149.

Hong, Y., Wang, H., Gao, Y., Bi, Y., Xiong, X., Yan, Y., Wang, J. *et al.* (2022) ERF transcription factor OsBIERF3 positively contributes to immunity against fungal and bacterial diseases but negatively regulates cold tolerance in rice. *Int. J. Mol. Sci.* **23**(2), 606.

Hu, Y.-T., Xu, Z.-C., Tian, Y., Gao, R.-R., Ji, A.-J., Pu, X.-D., Wang, Y. *et al.* (2020) Genome-wide identification and analysis of AP2/ERF transcription factors related to camptothecin biosynthesis in *Camptotheca acuminata*. *Chin. J. Nat. Med.* **18**(8), 582–593.

Hu, Y., Cheng, Y., Yu, X., Liu, J., Yang, L., Gao, Y., Ke, G. *et al.* (2021) Overexpression of two *CDPKs* from wild Chinese grapevine enhances powdery mildew resistance in *Vitis vinifera* and Arabidopsis. *New Phytol.* **230**(5), 2029–2046.

Huang, L., Zhang, S., Singer, S.D., Yin, X., Yang, J., Wang, Y. and Wang, X. (2016) Expression of the grape VqSTS21 gene in Arabidopsis confers resistance to osmotic stress and biotrophic pathogens but not *Botrytis cinerea*. *Front. Plant Sci.* **7**, 1379.

Huang, L., Yin, X., Sun, X., Yang, J., Rahman, M.Z., Chen, Z. and Wang, X. (2018) Expression of a grape VqSTS36-increased resistance to powdery mildew and osmotic stress in Arabidopsis but enhanced susceptibility to *Botrytis cinerea* in Arabidopsis and tomato. *Int. J. Mol. Sci.* **19**(10), 2985.

Huang, P.-Y., Zhang, J., Jiang, B., Chan, C., Yu, J.-H., Lu, Y.-P., Chung, K. *et al.* (2019) NINJA-associated ERF19 negatively regulates Arabidopsis pattern-triggered immunity. *J. Exp. Bot.* **70**(3), 1033–1047.

Jaillon, O., Aury, J.-M., Noel, B., Policriti, A., Clepet, C., Casagrande, A., Choisne, N. *et al.* (2007) The grapevine genome sequence suggests ancestral hexaploidization in major angiosperm phyla. *Nature* **449**(7161), 463–467.

Jang, M.S., Cai, L., Udeani, G.O., Slowing, K.V. and Pezzuto, J.M. (1997) Cancer chemopreventive activity of resveratrol, a natural product derived from grapes. *Science* **275**(5297), 218–220.

Jiang, J., Xi, H., Dai, Z., Lecourieux, F., Yuan, L., Liu, X., Patra, B. *et al.* (2019) VvWRKY8 represses stilbene synthase genes through direct interaction with VvMYB14 to control resveratrol biosynthesis in grapevine. *J. Exp. Bot.* **70**(2), 715–729.

Jiang, C., Wang, D., Zhang, J., Xu, Y., Zhang, C., Zhang, J., Wang, X. *et al.* (2021) VqMYB154 promotes polygene expression and enhances resistance to pathogens in Chinese wild grapevine. *Hortic. Res.* **8**(1), 151.

Jones, J.D.G. and Dangl, J.L. (2006) The plant immune system. *Nature* **444** (7117), 323–329.

Khattab, I.M., Sahi, V.P., Baltenweck, R., Maia-Grondard, A., Hugueney, P., Bieler, E., Dürrenberger, M. *et al.* (2021) Ancestral chemotypes of cultivated grapevine with resistance to Botryosphaeriaceae-related dieback allocate metabolism towards bioactive stilbenes. *New Phytol.* **229**(2), 1133–1146.

Koch, E. and Slusarenko, A. (1990) Arabidopsis is susceptible to infection by a downy mildew fungus. *Plant Cell* **2**(5), 437–445.

Koh, S., André, A., Edwards, H., Ehrhardt, D. and Somerville, S. (2005) *Arabidopsis thaliana* subcellular responses to compatible *Erysiphe cichoracearum* infections. *Plant J.* **44**(3), 516–529.

Leckband, G. and Lörz, H. (1998) Transformation and expression of a stilbene synthase gene of *Vitis vinifera* L. in barley and wheat for increased fungal resistance. *Theoretical & Applied Genetics* **96**(8), 1004–1012.

Li, R. (2019) *Regulation Mechanism of Stilbenes Metabolism in Chinese wild Vitis quinquangularis Using Multi-Omics Analysis*. Yangling: Northwest A & F University.

Li, T., Jiang, Z., Zhang, L., Tan, D., Wei, Y., Yuan, H., Li, T. *et al.* (2016) Apple (*Malus domestica*) MdERF2 negatively affects ethylene biosynthesis during fruit ripening by suppressing *MdACS1* transcription. *Plant J.* **88**(5), 735–748.

Li, X., Xu, Y., Shen, S., Yin, X., Klee, H., Zhang, B., Chen, K. *et al.* (2017) Transcription factor CitERF71 activates the terpene synthase gene *CitTPS16* involved in the synthesis of *E*-geraniol in sweet orange fruit. *J. Exp. Bot.* **68** (17), 4929–4938.

Li, Z., Wu, R., Guo, F., Wang, Y., Nick, P. and Wang, X. (2025) Advances in the molecular mechanism of grapevine resistance to fungal diseases. *Mol. Hortic.* **5**(1), 1.

Lin, T., Du, J., Zheng, X., Zhou, P., Li, P. and Lu, X. (2020) Comparative transcriptome analysis of MeJA-responsive AP2/ERF transcription factors involved in notoginsenosides biosynthesis. *3 Biotech.* **10**(7), 290.

Lipka, U., Fuchs, R. and Lipka, V. (2008) *Arabidopsis* non-host resistance to powdery mildews. *Curr. Opin. Plant Biol.* **11**(4), 404–411.

Liu, A.-C. and Cheng, C.-P. (2017) Pathogen-induced ERF68 regulates hypersensitive cell death in tomato. *Mol. Plant Pathol.* **18**(1), 1062–1074.

Liu, M., Ma, F., Wu, F., Jiang, C. and Wang, Y. (2019) Expression of stilbene synthase *VqSTS6* from wild Chinese *Vitis quinquangularis* in grapevine enhances resveratrol production and powdery mildew resistance. *Planta* **250** (6), 1997–2007.

Liu, W., Yan, C., Li, R., Chen, G., Wang, X., Wen, Y., Zhang, C. *et al.* (2023) VqMAPK3/VqMAPK6, VqWRKY33, and VqNSTS3 constitute a regulatory node in enhancing resistance to powdery mildew in grapevine. *Hortic. Res.* **10**(7), uhad116.

Livak, K.J. and Schmittgen, T.D. (2001) Analysis of relative gene expression data using real-time quantitative PCR and the 2(-Delta Delta C(T)) Method. *Methods* **25**(4), 402–408.

Lu, W., Deng, F., Jia, J., Chen, X., Li, J., Wen, Q., Li, T. *et al.* (2020) The *Arabidopsis thaliana* gene AtERF019 negatively regulates plant resistance to *Phytophthora parasitica* by suppressing PAMP-triggered immunity. *Mol. Plant Pathol.* **21**(9), 1179–1193.

Ma, R., Xiao, Y., Lv, Z., Tan, H., Chen, R., Li, Q., Chen, J. *et al.* (2017) AP2/ERF transcription factor, Ii049, positively regulates lignan biosynthesis in *Isatis indigotica* through activating salicylic acid signaling and Lignan/lignin pathway genes. *Front. Plant Sci.* **8**, 1361.

Ma, F., Wang, L. and Wang, Y. (2018) Ectopic expression of VpSTS29, a stilbene synthase gene from *Vitis pseudoreticulata*, indicates STS presence in cytosolic oil bodies. *Planta* **248**(1), 89–104.

Ma, H., Yang, T., Li, Y., Zhang, J., Wu, T., Song, T., Yao, Y. *et al.* (2021) The long noncoding RNA MdLNC499 bridges MdWRKY1 and MdERF109 function to regulate early-stage light-induced anthocyanin accumulation in apple fruit. *Plant Cell* **33**(10), 3309–3330.

Ma, L., Song, N., Duan, Q., Du, W., Li, X., Jia, W., Cui, G. *et al.* (2024) Jasmonate/ethylene- and NaWRKY6/3-regulated Alternaria resistance depends on ethylene response factor 1B-like in *Nicotiana attenuata*. *J. Exp. Bot.* **75**(20), 6593–6608.

Mehlhorn, D.G., Wallmeroth, N., Berendzen, K.W. and Grefen, C. (2018) 2in1 vectors improve in planta BiFC and FRET analyses. *Methods Mol. Biol.* **1691**, 139–158.

Meyer, D., Pajonk, S., Micali, C., O'Connell, R. and Schulze-Lefert, P. (2009) Extracellular transport and integration of plant secretory proteins into pathogen-induced cell wall compartments. *Plant J.* **57**(6), 986–999.

Micali, C., Göllner, K., Humphry, M., Consonni, C. and Panstruga, R. (2008) The powdery mildew disease of *Arabidopsis*: a paradigm for the interaction between plants and biotrophic fungi. *Arabidopsis Book* **6**, e0115.

Micali, C.O., Neumann, U., Grunewald, Panstruga, R. and O'Connell, R. (2011) Biogenesis of a specialized plant-fungal interface during host cell internalization of *Golovinomyces orontii* haustoria. *Cell. Microbiol.* **13**(2), 210–226.

Mu, H., Li, Y., Yuan, L., Jiang, J., Wei, Y., Duan, W., Fan, P. *et al.* (2023) MYB30 and MYB14 form a repressor-activator module with WRKY8 that controls stilbene biosynthesis in grapevine. *Plant Cell* **35**(1), 552–573.

Nelson, B.K., Cai, X. and Nebenführ, A. (2007) A multicolored set of in vivo organelle markers for co-localization studies in Arabidopsis and other plants. *Plant J.* **51**(6), 1126–1136.

Orduña, L., Li, M., Navarro-Payá, D., Zhang, C., Santiago, A., Romero, P., Ramšak, Ž. *et al.* (2022) Direct regulation of shikimate, early phenylpropanoid and stilbenoid pathways by Subgroup 2 R2R3-MYBs in grapevine. *Plant J.* **110** (2), 529–547.

Pan, Q.H., Lei, W. and Li, J.M. (2009) Amounts and subcellular localization of stilbene synthase in response of grape berries to UV irradiation. *Plant Sci.* **176** (3), 360–366.

Parage, C., Tavares, R., Réty, S., Baltenweck-Guyot, R., Poutaraud, A., Renault, L., Heintz, D. *et al.* (2012) Structural, functional, and evolutionary analysis of the unusually large stilbene synthase gene family in grapevine. *Plant Physiol.* **160**(3), 1407–1419.

Paul, P., Singh, S.K., Patra, B., Sui, X., Pattanaik, S. and Yuan, L. (2017) A differentially regulated AP2/ERF transcription factor gene cluster acts downstream of a MAP kinase cascade to modulate terpenoid indole alkaloid biosynthesis in *Catharanthus roseus*. *New Phytol.* **213**(3), 1107–1123.

Pezet, R., Gindro, K., Viret, O. and Spring, J.L. (2004) Glycosylation and oxidative dimerization of resveratrol are respectively associated to sensitivity and resistance of grapevine cultivars to downy mildew. *Physiol. Mol. Plant Pathol.* **65**(6), 297–303.

Pillai, S.E., Kumar, C., Dasgupta, M., Kumar, B.K., Vungarala, S., Patel, H.K. and Sonti, R.V. (2020) Ectopic expression of a cell-wall-degrading enzyme-induced *OsAP2/ERF152* leads to resistance against bacterial and fungal infection in Arabidopsis. *Phytopathology* **110**(4), 726–733.

Pruitt, R.N., Gust, A.A. and Nurnberger, T. (2021) Plant immunity unified. *Nat. Plants* **7**(4), 382–383.

Qiu, W., Feechan, A. and Dry, I. (2015) Current understanding of grapevine defense mechanisms against the biotrophic fungus (*Erysiphe necator*), the causal agent of powdery mildew disease. *Hortic. Res.* **2**, 15020.

Ramming, D.W., Gabler, F., Smilanick, J., Cadle-Davidson, M., Barba, P., Mahanil, S. and Cadle-Davidson, L. (2010) A single dominant locus, *Ren4*, confers rapid non-race-specific resistance to grapevine powdery mildew. *Phytopathology* **101**(4), 502–508.

Rubiato, H.M., Liu, M., O'Connell, R.J. and Nielsen, M.E. (2022) Plant SYP12 syntaxins mediate an evolutionarily conserved general immunity to filamentous pathogens. *elife* **11**, e73487.

Schnee, S., Viret, O. and Gindro, K. (2008) Role of stilbenes in the resistance of grapevine to powdery mildew. *Physiol. Mol. Plant Pathol.* **72**(4-‐6), 128–133.

Schöppner, A. and Kindl, H. (1984) Purification and properties of a stilbene synthase from induced cell suspension cultures of peanut. *J. Biol. Chem.* **259** (11), 6806–6811.

Sedgwick, P. (2012) Pearson's correlation coefficient. *Br. Med. J.* **344**, e4483.

Shi, J., He, M., Cao, J., Wang, H., Ding, J., Jiao, Y., Li, R. *et al.* (2014) The comparative analysis of the potential relationship between resveratrol and stilbene synthase gene family in the development stages of grapes (*Vitis quinquangularis* and *Vitis vinifera*). *Plant Physiol. Biochem.* **74**, 24–32.

Song, J., Chen, C., Zhang, S., Wang, J., Huang, Z., Chen, M., Cao, B. *et al.* (2020) Systematic analysis of the Capsicum ERF transcription factor family: identification of regulatory factors involved in the regulation of species-specific metabolites. *BMC Genomics* **21**(1), 573.

Stark-Lorenzen, P., Nelke, B., Hänßler, G., Mühlbach, H.P. and Thomzik, J.E. (1997) Transfer of a grapevine stilbene synthase gene to rice (*Oryza sativa* L.). *Plant Cell Rep.* **16**(10), 668–673.

Tan, H., Xiao, L., Gao, S., Li, Q., Chen, J., Xiao, Y., Ji, Q. *et al.* (2015) *TRICHOME AND ARTEMISININ REGULATOR* 1 is required for trichome development and artemisinin biosynthesis in *Artemisia annua* L. *Mol. Plant* **8**(9), 1396–1411.

Thomzik, J.E., Stenzel, K., Stcker, R., Schreier, P.H. and Stahl, D.J. (1997) Synthesis of a grapevine phytoalexin in transgenic tomatoes (*Lycopersicon esculentum* Mill.) conditions resistance against *Phytophthora* infestans. *Physiol. Mol. Plant Pathol.* **51**(4), 265–278.

Thordal-Christensen, H., Zhang, Z., Wei, Y. and Collinge, D.B. (1997) Subcellular localization of H_2O_2 in plants. H_2O_2 accumulation in papillae and hypersensitive response during the barley—powdery mildew interaction. *Plant J.* **11**(6), 1187–1194.

Vannozzi, A., Dry, I.B., Fasoli, M., Zenoni, S. and Lucchin, M. (2012) Genome-wide analysis of the grapevine stilbene synthase multigenic family: genomic organization and expression profiles upon biotic and abiotic stresses. *BMC Plant Biol.* **12**, 1471–2229.

Vannozzi, A., Wong, D.C.J., Höll, J., Hmmam, I., Matus, J.T., Bogs, J., Ziegler, T. *et al.* (2018) Combinatorial regulation of stilbene synthase genes by WRKY and MYB transcription factors in grapevine (*Vitis vinifera* L.). *Plant Cell Physiol.* **59**(5), 1043–1059.

Vishnevetsky, J., TLW, J., Palmateer, A.J., Flaishman, M., Cohen, Y., Elad, Y., Velcheva, M. *et al.* (2011) Improved tolerance toward fungal diseases in transgenic *Cavendish banana* (Musa spp. AAA group) cv. grand nain. *Transgenic Res.* **20**(1), 61–72.

Waadt, R., Schmidt, L.K., Lohse, M., Hashimoto, K., Bock, R. and Kudla, J. (2010) Multicolor bimolecular fluorescence complementation reveals simultaneous formation of alternative CBL/CIPK complexes in planta. *Plant J.* **56**(3), 505–516.

Wang, L. and Wang, Y. (2019a) Transcription factor VqERF114 regulates stilbene synthesis in Chinese wild *Vitis quinquangularis* by interacting with VqMYB35. *Plant Cell Rep.* **38**(10), 1347–1360.

Wang, Y., Liu, Y., HE, P., Chen, J., Lamikanra, O. and Lu, J. (1995) Evaluation of foliar resistance to *Uncinula necator* in Chinese wild *Vitis* spp. species. *Vitis* **34** (3), 159–164.

Wang, Y., Wang, D., Wang, F., Huang, L., Tian, X., Sv, N., Gao, H. *et al.* (2017) Expression of the Grape *VaSTS19* gene in *Arabidopsis* improves resistance to powdery mildew and *Botrytis cinerea* but increases susceptibility to *Pseudomonas syringe* pv tomato DC3000. *Int. J. Mol. Sci.* **18**(9), 2000.

Wang, M., Zhu, Y., Han, R., Yin, W., Guo, C., Li, Z. and Wang, X. (2018) Expression of *Vitis amurensis VaERF20* in *Arabidopsis thaliana* improves resistance to *Botrytis cinerea* and *Pseudomonas syringae* pv. Tomato DC3000. *Int. J. Mol. Sci.* **19**(3), 696.

Wang, X., Zeng, W., Ding, Y., Wang, Y., Niu, L., Yao, J.-L., Pan, L. *et al.* (2019) Peach ethylene response factor PpeERF2 represses the expression of ABA biosynthesis and cell wall degradation genes during fruit ripening. *Plant Sci.* **283**, 116–126.

Wang, D., Jiang, C., Liu, W. and Wang, Y. (2020a) The WRKY53 transcription factor enhances stilbene synthesis and disease resistance by interacting with MYB14 and MYB15 in Chinese wild grape. *J. Exp. Bot.* **71**(10), 3211–3226.

Wang, J.-H., Gu, K.-D., Han, P.-L., Yu, J.-Q., Wang, C.-K., Zhang, Q.-Y., You, C.-X. *et al.* (2020b) Apple ethylene response factor MdERF11 confers resistance to fungal pathogen *Botryosphaeria dothidea*. *Plant Sci.* **291**, 110351.

Wang, Y., Jiang, H., Mao, Z., Liu, W., Jiang, S., Xu, H., Su, M. *et al.* (2021) Ethylene increases the cold tolerance of apple via the MdERF1B-MdCIbHLH1 regulatory module. *Plant J.* **106**(2), 379–393.

Wen, Y., Wang, W., Feng, J., Luo, M.C., Tsuda, K., Katagiri, F., Bauchan, G. *et al.* (2011) Identification and utilization of a sow thistle powdery mildew as a poorly adapted pathogen to dissect post-invasion non-host resistance mechanisms in *Arabidopsis*. *J. Exp. Bot.* **62**(6), 2117–2129.

Weßling, R. and Panstruga, R. (2012) Rapid quantification of plant-powdery mildew interactions by qPCR and conidiospore counts. *Plant Methods* **8**(1), 35.

Wong, D.C.J., Schlechter, R., Vannozzi, A., Höll, J., Hmmam, I., Bogs, J., Tornielli, G.B. *et al.* (2016) A systems-oriented analysis of the grapevine R2R3-MYB transcription factor family uncovers new insights into the regulation of stilbene accumulation. *DNA Res.* **23**(5), 451–466.

Wu, X., Wang, L., Xing, Q., Zhao, Y. and Qi, H. (2024) CmPIF8-CmERF27-CmACS10-mediated ethylene biosynthesis modulates red light-induced powdery mildew resistance in oriental melon. *Plant Cell Environ.* **47**(11), 4135–4150.

Xiang, G., Fan, Z., Lan, S., Wei, D., Gao, Y., Kang, H. and Yao, Y. (2025) Ethylene increases the NaHCO$_3$ stress tolerance of grapevines partially via the VvERF1B-VvMYC2-VvPMA10 pathway. *Plant Biotechnol. J.* https://doi.org/10.1111/pbi.14565

Xie, Y., Chen, P., Yan, Y., Bao, C., Li, X., Wang, L., Shen, X. *et al.* (2018) An atypical R2R3 MYB transcription factor increases cold hardiness by CBF-dependent and CBF-independent pathways in apple. *New Phytol.* **218**(1), 201–218.

Xu, W., Ma, F., Li, R., Zhou, Q., Yao, W., Jiao, Y., Zhang, C. *et al.* (2019a) VpSTS29/STS2 enhances fungal tolerance in grapevine through a positive feedback loop. *Plant Cell Environ.* **42**(11), 2979–2998.

Xu, S., Yao, S., Huang, R., Tan, Y. and Huang, D. (2020) Transcriptome-wide analysis of the *AP2/ERF* transcription factor gene family involved in the regulation of gypenoside biosynthesis in *Gynostemma pentaphyllum*. *Plant Physiol. Biochem.* **154**, 238–247.

Yan, C., Yang, N., Li, R., Wang, X., Xu, Y., Zhang, C., Wang, X. *et al.* (2023) Alfin-like transcription factor VqAL4 regulates a stilbene synthase to enhance powdery mildew resistance in grapevine. *Mol. Plant Pathol.* **24**(2), 123–141.

Yao, W., Wang, L., Wang, J., Ma, F., Yang, Y., Wang, C., Tong, W. *et al.* (2017) VpPUB24, a novel gene from Chinese grapevine, *Vitis pseudoreticulata*, targets VpICE1 to enhance cold tolerance. *J. Exp. Bot.* **68**(11), 2933–2949.

Yin, W., Wang, X., Liu, H., Wang, Y., Nocker, S., Tu, M., Fang, J. *et al.* (2022) Overexpression of *VqWRKY31* enhances powdery mildew resistance in grapevine by promoting salicylic acid signaling and specific metabolite synthesis. *Hort Res.* **9**, uhab064.

Zang, Z., Lv, Y., Liu, S., Yang, W., Ci, J., Ren, X., Wang, Z. *et al.* (2020) A novel ERF transcription factor, *ZmERF105*, positively regulates maize resistance to *Exserohilum turcicum*. *Front. Plant Sci.* **11**, 850.

Zang, Z., Wang, Z., Zhao, F., Yang, W., Ci, J., Ren, X., Jiang, L. *et al.* (2021) Maize ethylene response factor *ZmERF061* is required for resistance to *Exserohilum turcicum*. *Front. Plant Sci.* **12**, 630413.

Zhang, Y., Ji, A., Xu, Z., Luo, H. and Song, J. (2019) The AP2/ERF transcription factor SmERF128 positively regulates diterpenoid biosynthesis in *Salvia miltiorrhiza*. *Plant Mol. Biol.* **100**(1–2), 83–93.

Zhang, C., Gao, H., Sun, Y., Jiang, L., He, S., Song, B., Liu, S. *et al.* (2021) The BTB/POZ domain protein GmBTB/POZ promotes the ubiquitination and degradation of the soybean AP2/ERF-like transcription factor GmAP2 to regulate the defense response to *Phytophthora sojae*. *J. Exp. Bot.* **72**(22), 7891–7908.

Zhao, F., Li, Y., Hu, Y., Gao, Y., Zang, X., Ding, Q., Wang, Y. *et al.* (2016) A highly efficient grapevine mesophyll protoplast system for transient gene expression and the study of disease resistance proteins. *Plant Cell Tissue Organ Cult.* **125**, 43–57.

Zhao, C., Liu, X., Gong, Q., Cao, J., Shen, W., Yin, X., Grierson, D. *et al.* (2021) Three AP2/ERF family members modulate flavonoid synthesis by regulating type IV chalcone isomerase in citrus. *Plant Biotechnol. J.* **19**(4), 671–688.

Zheng, H., Jing, L., Jiang, X., Pu, C., Zhao, S., Yang, J., Guo, J. *et al.* (2021) The ERF-VII transcription factor SmERF73 coordinately regulates tanshinone biosynthesis in response to stress elicitors in *Salvia miltiorrhiza*. *New Phytol.* **231**(5), 1940–1955.

Zhou, Q., Dai, L., Cheng, S., He, J., Wang, D., Zhang, J. and Wang, Y. (2014) A circulatory system useful both for long-term somatic embryogenesis and genetic transformation in *Vitis vinifera* L. cv. Thompson seedless. *Plant Cell Tissue Organ Cult.* **118**(1), 157–168.

Zhou, Q., Du, Y., Cheng, S., Li, R., Zhang, J. and Wang, Y. (2015) Resveratrol derivatives in four tissues of six wild Chinese grapevine species. *N. Z. J. Crop. Hortic. Sci.* **43**, 204–213.

Zhu, Y.J., Agbayani, R., Jackson, M.C., Tang, C.S. and Moore, P.H. (2004) Expression of the grapevine stilbene synthase gene *VST1* in papaya provides increased resistance against diseases caused by *Phytophthora palmivora*. *Planta* **220**(2), 241–250.

Zhu, K., Sun, Q., Chen, H., Mei, X., Lu, S., Ye, J., Chai, L. *et al.* (2021) Ethylene activation of carotenoid biosynthesis by a novel transcription factor CsERF061. *J. Exp. Bot.* **72**(8), 3137–3154.

Zhuang, M., Li, C., Wang, J., Mao, X., Li, L., Yin, J., Du, Y. *et al.* (2021) The wheat *SHORT ROOT LENGTH 1* gene TaSRL1 controls root length in an auxin-dependent pathway. *J. Exp. Bot.* **72**(20), 6977–6989.

Supporting information

Additional supporting information may be found online in the Supporting Information section at the end of the article.

Figure S1 HPLC-MS mass spectrogram.
Figure S2 Detection of *VqNSTS2* transgenic grapevine plants.
Figure S3 Screening of the potential regulation factors of *VqNSTS2*.
Figure S4 Sequence analysis of *VqERF062* isolated from Chinese wild *Vitis quinquangularis* accession Danfeng-2.
Figure S5 VqERF062 has transcriptional activation activity in yeast.
Figure S6 VqERF062 interacts with itself.
Table S1 Determination of the content of stilbenes.
Table S2 Co-expression transcription factors with *VqNSTS2*.
Table S3 List of the VqERF062-interacting proteins.
Table S4 List of all primers used in this study.